TIME-DOMAIN ANALYSIS OF AN UWB PULSE DISTORTION IN WIRELESS CHANNEL

DISSERTATION

SUBMITTED IN PARTIAL FULFILLMENT OF THE REQUIREMENTS
FOR THE AWARD OF THE DEGREE
OF

MASTER OF TECHNOLOGY
IN
SIGNAL PROCESSING & DIGITAL DESIGN

Submitted by:

Rahul Kumar Jaiswal

2K12/SPD/14

Under the supervision of

Dr. S.K. Soni

DEPARTMENT OF ELECTRONICS & COMMUNICATION ENGINEERING
DELHI TECHNOLOGICAL UNIVERSITY
(Formerly Delhi College of Engineering)
Bawana Road, Delhi-110042

2014

CERTIFICATE

DELHI TECHNOLOGICAL UNIVERSITY
(Formerly Delhi College of Engineering)
BAWANA ROAD, DELHI – 110042
Department of Electronics & Communication Engineering

This is to certify that the thesis titled **"Time-Domain Analysis of an UWB Pulse Distortion in Wireless Channel"** submitted by Rahul Kumar Jaiswal, Roll. No. 2K12/SPD/14, in partial fulfillment for the award of degree of Master of Technology in Signal Processing & Digital Design at **Delhi Technological University, Delhi**, is a bonafide record of student's own work carried out by him under my supervision and guidance in the academic session 2013-14. The matter embodied in dissertation has not been submitted for the award of any other degree or certificate in this or any other university or institute.

(Dr. S. K. Soni)

ASSOCIATE PROFESSOR
Department of Electronics & Communication Engineering
Delhi Technological University,
(Formerly Delhi College of Engineering)
Delhi -110042

ACKNOWLEDGEMENT

I express my sincere gratitude to my guide **Dr. S.K. Soni** for giving valuable suggestion during the course of the investigation, for his ever encouraging and moral support. His enormous knowledge and investigation always helped me unconditionally to solve various problems. I would like to thank him for introducing me with the problem and providing valuable advice throughout the course of work. I truly admire his depth of knowledge and strong dedication to students and research that has made him one of the most successful professors ever. His mastery of any topic is amazing, but yet he is such a humble and down to earth person. I am glam that I was given opportunity to work with him. He surely brings out the best in his students.

I am greatly thankful to **Prof. Rajiv Kapoor, Professor and Head,** Department of Electronics & Communication Engineering, entire faculty and staff of electronics & Communication Engineering for their, continuous support, encouragement and inspiration in the execution of this "**thesis"** work.

I would like to thank my parents who bestowed upon me their grace and were source of my inspiration and encouragement.

I am thankful to almighty god his grace and always with me whenever I felt lonely.I am also thankful to my classmates for their continious support and helpfullness whenever it is needed.

Rahul Kumar Jaiswal

ABSTRACT

An accurate time-domain (TD) modeling for transmission of UWB signal through a 3-dimensional building structure made of low loss dielectric materials is presented. Transmission through building is analyzed for arbitrary position of transmitter and receiver. Time-domain formulation are presented for transmission coefficient for both soft and hard polarizations, for propagation loss and then for the transmitted field at the receiver. An analytical time domain (TD) solution, based on an established FD diffraction model, is also presented for diffraction of UWB signal through same dielectric obstacle.

The comparison of transmitted and reflected field proves that the transmitted field component is very significant in case of non line of sight (NLOS) communication in deep shadow regions, where the reflected and diffracted components are weak. The TD results have been validated with the inverse fast Fourier transform (IFFT) of the corresponding exact frequency domain results. The significant gain in the computational speed achieved through the proposed TD method is demonstrated by comparing its computation time with that of the exact IFFT-FD solution. Finally comparative analysis of normalized mean and mean square error between both methods is performed for different loss tangent values. It is shown that the proposed TD solution outperforms the exact IFFT-FD solution in terms of computational efficiency. Also it is observed that normalized error tends to increase for higher loss tangent values.

Table of Contents

LIST OF FIGURES

LIST OF TABLES

LIST OF ABBREVIATIONS USED

UWB	ULTRA-WIDEBAND
FD	FREQUENCY-DOMAIN
TD	TIME-DOMAIN
IFFT-FD	INVERSE FAST FOURIER TRANSFORM OF FREQUENCY DOMAIN
UTD	UNIFORM THEORY OF DIFFRACTION
GTD	GEOMETRICAL THEORY OF DIFFRACTION
SP	SOFT POLARIZATION
HP	HARD POLARIZATION
PC	PERFECTLY CONDUCTING
Tx	TRANSMITTER
Rx	RECEIVER
NS	NANO SECOND

Chapter 1

INTRODUCTION

The promise of Ultra-Wideband Communication for high speed connectivity, greater data rate, lower hardware cost, and lower complexity in system are the main reason for increasing interest in the study of Ultra wide-band communication. As it is clear from the name, Ultra Wide-band means a large band of frequencies.

1.1 Motivation

This study deals with the problem of accurate prediction of the ultra wide-band channel. Due to huge Band-Width for a UWB signal, all the basic principles of propagation models need to be re-examined. The propagation of UWB signals in indoor/outdoor environments is one of the key issues with significant impacts on the future direction, scope, and the extent of the success of UWB technology.

UWB communication systems employ very short duration pulses, which are usually 1 ns wide, for both transmission and reception. Therefore, UWB signals are very flexible to the multipath phenomena. Due to its limit on PSD (imposed by FCC) its PSD is very low and it is received by other communication system as noise. In the narrow band communication, the response of the channel to the noise is nearly flat, and that is why the distortion in the signal is very nominal. The shape of received signal is almost unaffected for a narrow band signal over transmission through a channel. For UWB communication, since the BW of the UWB pulse is extremely large and each multipath component is frequency dependent with its own impulse response of each multipath component. Thus, the receiver receives a distorted pulse after transmission through a channel. UWB signals employ many advantages such as: (i) Accurate position location (ii) multiple access due to wide transmission bandwidths (iii) possibility of extremely high data rates (iv) possible easier material penetration, due to presence of energy at different frequencies. For realizing such a system that is so much efficient we need to properly estimate the channel so that the distortion in the signal can be known. Also the knowledge of UWB pulse distortion helps to design the matched filter and Rake receiver optimally. There are two approaches which is used in order to analyze the distortion in the UWB pulse: (i) First

obtain frequency-domain (FD) solution of the propagation channel and then taking IFFT of the results obtained (ii) Direct time-domain (TD) solution. Since UWB signal has a very broad frequency range, it is very computationally inefficient to apply the former approach to determine the frequency response of the channel and so its pulse distortion [1]. It is more convenient to work directly in time-domain. Moreover, with the help of the TD approach of the uniform theory of diffraction (UTD), the impulse response of the channel model can be calculated and it is convolved with the transmitted pulse to predict the received signals. All the detailed features which are of importance in the UWB system, such as the time delay, the power and the pulse shape/distortion can be obtained very easily with the help of TD approach. It is also helpful in determining time delay parameters of the wireless channel which is of great importance in application involving synchronization, positioning and detection.

1.2 Overview of UWB wireless Communication System

Ultra-wideband (UWB) has emerged as a technology that offers great promise to satisfy the growing demand for low-cost, high speed digital wireless indoor and home networks. UWB signals are defined as signals with either a large relative bandwidth (typically, larger than 20%), or a large absolute bandwidth (> 500 MHz). This large bandwidth leads to new possibilities for both communications and radar applications. This technology is different from conventional narrowband wireless transmission technology-instead of broadcasting on separate frequencies; UWB spreads signals across a very wide range of frequencies. The typical sinusoidal radio wave is replaced by train of pulses per second.

1.2.1 Definition of UWB

Ultra-wideband (UWB) is a technology that uses short duration (picoseconds to nanoseconds) pulse for transmission and reception of information. Since frequency is inversely related to time, short duration UWB pulses spread their energy across a wide range of frequencies from near DC to several gigahertz (GHz) with very low power spectral density (PSD). The average transmission power of a UWB system is very low (in order of microwatts) due to low duty cycle short-duration UWB pulses. According to FCC's definition, UWB signals must have bandwidths of greater than 500 MHz or a fractional bandwidth greater than 20 percent.

Fractional bandwidth is factor which is used to classify signals as narrowband, wideband or ultra wideband and it is defined by the ratio of bandwidth at 10 dB points to the center frequency and is given as:

$$B_f = \frac{BW}{f_c} = \frac{(f_H - f_L)}{(f_H + f_L)/2} \tag{1.1}$$

Where f_H and f_L are highest and lowest cut off frequencies (at 10 dB points) of a UWB pulse spectrum, respectively, f_c is the center frequency and BW is the signal bandwidth.

1.2.2 Advantage of UWB

UWB technology uses short-duration pulses and it offers several advantages over narrowband communication systems. The main advantages of UWB technology are:

- **High Data rate:** One of the major advantages for UWB pulses of large bandwidth is improved channel capacity. Data rate, or channel capacity is defined as the maximum amount of data that can be transmitted per second over a communications channel. Higher data rates can enable new applications and devices that would not have been possible up until now. Speeds of over 100 Mbps have been demonstrated, and the potential for higher speeds over short distances is there. This high data rate can be explained by examining Shannon's famous capacity equation [5] given by:

$$C = B\log\left(1+\frac{S}{N}\right) \tag{1.2}$$

Where C is the maximum channel capacity(bits/second), B is the channel bandwidth (Hz), S is the signal power (W) and N is the noise power (W). It can be seen from this equation that the capacity of a channel grows linearly with increasing bandwidth B, but only logarithmically with signal power S. UWB channel has an abundance of bandwidth and thus high data rate.

- **Simple Transceiver Architecture:** The conventional sinusoidal transmitters and receivers need a carrier signal for transmission of original message signal. UWB transmission is carrier-less, there is no need for mixtures and local oscillators to translate the carrier frequency to the required frequency band. The low component count leads to reduced cost, and smaller chip sizes lead to low-cost systems.

The simplest UWB transmitter could be assumed to be a pulse generator, a timing circuit, and an antenna. In Ultra-wideband communication, Because of transmission of low powered pulses, there is no need for power amplifier in UWB transmitters. These facts can reduce cost, size, weight, and power consumption of UWB systems compared with conventional narrowband communication systems.

- **High Performance in Multi Path Channel:** The multipath phenomenon is unavoidable in wireless communication. Multipath effect is caused by reflection, scattering and diffraction of electromagnetic energy by objects in-between the transmitter and the receiver. UWB pulses are extremely short, so they can be filtered or ignored. They can readily be distinguished from unwanted multipath reflections because of the fine time resolution. This leads to the characteristics of multipath immunity. The narrow pulses used by UWB, if separated out provide a fine resolution of reflected pulses at the receiver. This is important in any wireless communication, as pulses (or sinusoids) interfering with each other are the major obstacles to error-free communication. In UWB, if narrow pulses are separated by at least one pulse width they will not interfere. Assuming one symbol per pulse, they will not produce interference with the same symbol.

- **Ability to work with low Signal-to-Noise Ratios:** According to Hartley-Shannon formula which was given in equation 1, the channel capacity is only logarithmically dependent on signal to noise ratio. Therefore, UWB communication systems are capable of working in harsh communication channels with low SNRs and still offer a large channel capacity as a result of their large bandwidth.

1.2.3 Basic properties of UWB signals and systems :

- **Pulse Shape:** Ultra wideband system is baseband technology and its spectrum is determined by pulse shape and pulse width. UWB pulse shape consists of two factors. First factor minimize the power spectral density and interference by spreading the energy in frequency domain. Second one is used to avoid a dc component to maintain the antenna radiation efficiency. The Gaussian doublet pulse shown in fig.1.1 is often used in UWB system because its shape is easily generated.

It is simply a square pulse which has been shaped by the limited rise and fall times of the pulse and the filtering effects of transmit and receive antennas. A square pulse can be easily generated by switching a transistor on and off quickly. UWB pulses are typically of nanoseconds or picoseconds order.

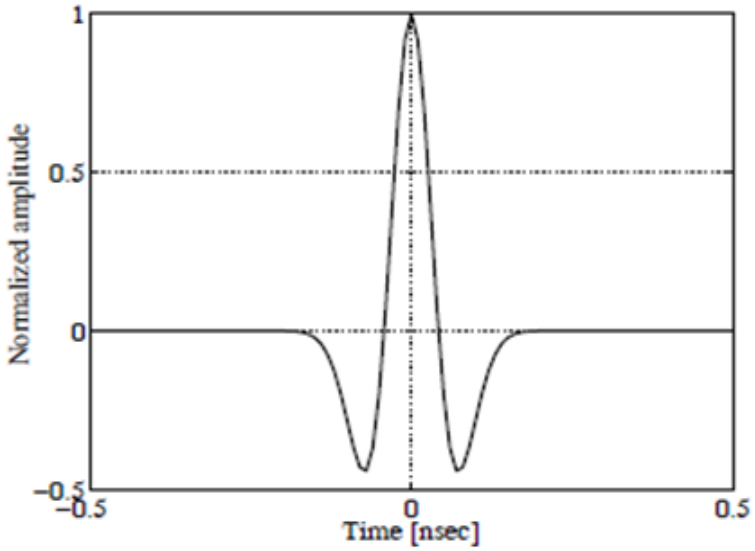

Fig 1.1 Idealized received UWB pulse

The fast switching on and off leads to a pulse shape which is not rectangular, but has the edges smoothed off. The pulse shape approximates the Gaussian function curve. Transmitting the pulses directly to the antennas will result in the pulses being filtered due to the properties of the antennas. The filtering operation can be modeled as a derivative operation. The same effect occurs at the receiver antenna.

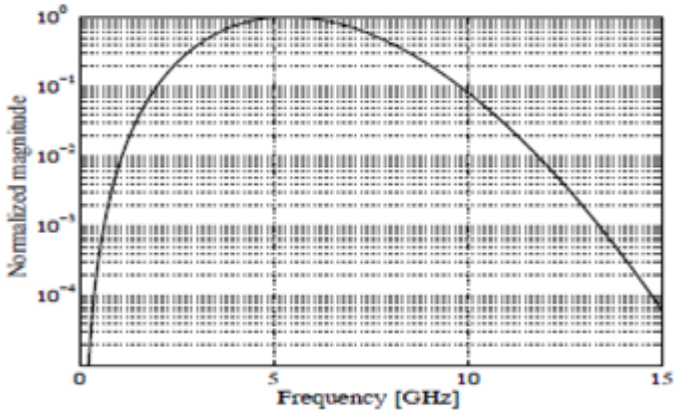

Fig. 1.2 Idealized spectrum of a single received UWB pulse.

The spectrum of the Gaussian doublet is shown in Fig. 1.2. The centre frequency can be seen to be approximately 5 GHz, with the 3 dB bandwidth extending over several GHz. In comparison with narrowband or even wideband communication systems the large bandwidth is evident and, hence the name UWB communication can easily by inferred.

- **Power spectral density (PSD):** The power spectral density (PSD) of UWB systems is considered to be extremely low, especially for communication applications. The PSD is defined as:

$$PSD = \frac{P}{B} \tag{1.3}$$

Where P is the power transmitted in watts (W), B is the bandwidth of the signal in hertz (Hz), and the unit of PSD is watts/hertz (W/Hz). For a UWB system the pulses have a short time duration t and very wide bandwidth B. One of the benefits of low-PSD is a low probability of detection, which is of particular interest for military applications. This is also a concern for wireless consumer applications, where the security of data for corporations and individual is of great concern.

- **Spectral Mask:** Since UWB occupies such a wide bandwidth, there are many users whose spectrum will be affected and need to be convinced that UWB will not cause undue interference to their existing services.

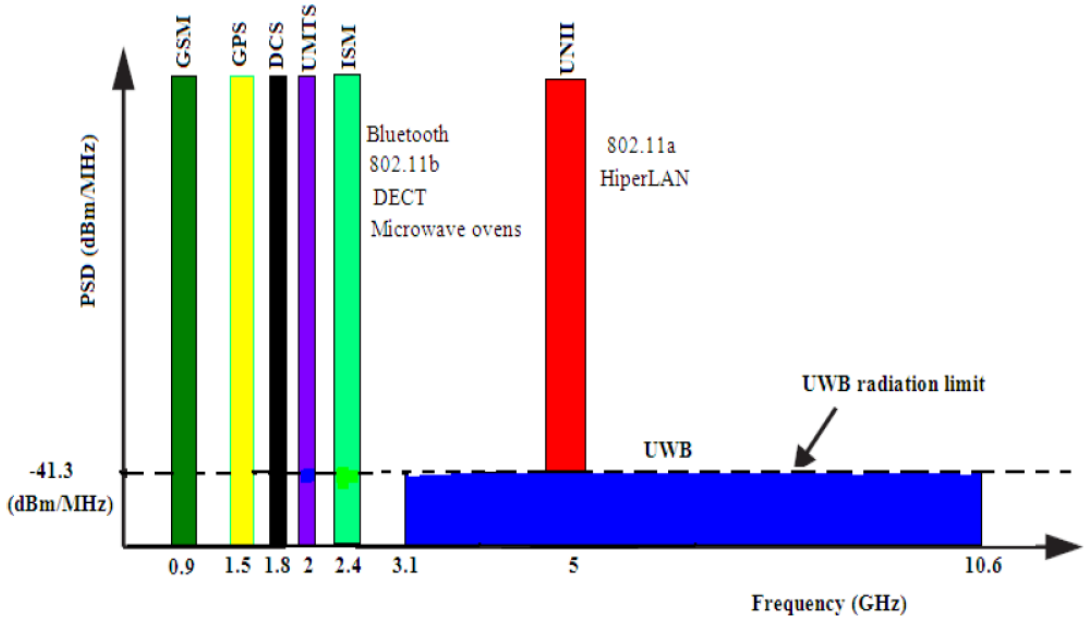

Fig 1.3 The spectrum of the UWB signals versus conventional signals

Federal Communications Commission (FCC) and other regulatory groups specify spectral masks for different applications which show the allowed power output for specific frequencies to keep the UWB interference with others users at minimum level**.** There are many systems, whether licensed or not, are present in UHF and SHF bands. Fig 1.3 shows that several radio system existing in UHF and SHF bands. Each frequency band has assigned the effective isotropic radiated power (EIRP) by the Federal Communication Commission (FCC).

Fig 1.4 shows FCC radiation limit for the indoor UWB communication system. A large continuous bandwidth of 7.5 GHz is available between 3.1 GHz and 10.6 GHz at a maximum power output of -41.3 dBm/MHz. Such power restriction allow UWB system to reside below the noise floor of a typical narrowband receiver and enables UWB to limit interference to existing communication systems and to protect the existing communication system.

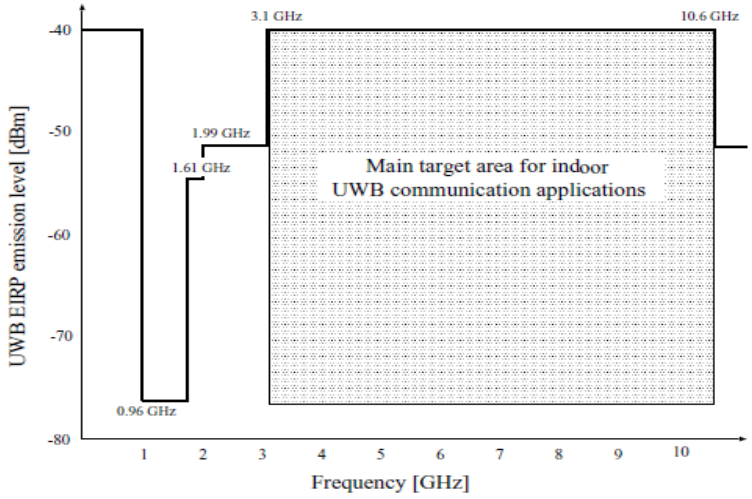

Fig 1.4 Spectral mask mandated by FCC for indoor UWB systems.

- **High Special capacity:** Spatial capacity, measured in bits per second per square meter (bps/m^2) is another important property of UWB systems. This term stems from the interest in even higher data rate, even over extremely short distances. Special capacity can be defined as the ratio of maximum data rate of a system to the area over which the system can transmit.

- **Superior Penetration Properties:** UWB system can penetrate effectively through different materials. UWB pulses are composed of a large range of frequencies and wavelength decreases with increase in frequency, thus the lower frequency components of UWB frequency spectrum have long wavelengths, which allow UWB signals to penetrate a variety of materials. Because of this penetration property, UWB systems can operate under both line of sight (LOS) and non-LOS (NLOS) conditions.

- **Security:** Because of their low average transmission power, UWB communications systems have an inherent immunity to detection and intercept.

- **High precision ranging:** UWB systems have good time-domain resolution and can promise sub-centimeter resolution capability for location and tracking applications.

1.2.4 Application of UWB

UWB technology can enable a wide variety of applications in wireless communications, radar imaging, networking, and localization system. Use of UWB technology under the FCC guidelines offers significant potential for the deployment of two basic communications systems in wireless communication.

- **High-data-rate short-range communications**: The high-data-rate wireless personal area networks (WPANs) can be defined as networks with a medium density of active devices per room (5 to 10) transmitting at data rates ranging from 100 to 500 Mbps within a distance of 20 m. The exceptionally large bandwidth available in UWB signal enables various WPAN applications, such as high-speed wireless universal serial bus (WUSB) connectivity for personal computers (PCs) and PC peripherals, file exchange among storage systems, and cable replacement for home entertainment systems.

- **Low-data-rate and long range communications**: Under the low-rate operation mode, UWB technology could be beneficial and potentially useful in sensor, positioning, and identification networks over relatively long range. A sensor network comprises a large number of nodes spread over a geographical area to be monitored. Depending on the specific application, the sensor nodes can be static or mobile. Key requirements for sensor networks operating in challenging environments include low cost, low powers, and

multi-functionality. UWB technology has unique properties like low complexity, low cost and low power. So UWB technology is well suited to sensor network applications. Moreover, due to the fine time resolution of UWB signals UWB-based sensing has the potential to improve the resolution of conventional proximity and motion sensors. The low-rate transmission, combined with accurate location tracking capabilities, offers an operational mode known as low-data-rate and location tracking.

- **Medical Applications**

UWB signals are not influenced by clothes or blankets, and can even penetrate human body, walls, ground, ice, mud, and many interesting potential applications for UWB in medicine can be envisioned. Hospitals, Operation theatres, Home health care, intensive care units (ICU), pediatric clinics, rescue operations (to look for heart beat under ruins, or soil, or snow) are few potential areas of application [6]. A UWB sensor network frees the patient from the tangle of wired sensors. Sensors are being used in medical situation to determine pulse rate, temperature, and other critical life signs. UWB is used to transport the sensor information without wires, but also function as a sensor of respiration, heart beats, and in some instance for medical imaging.

1.3 LITERAURE SURVEY

Efficient and reliable propagation model can optimize the network planning and reduce unnecessary interference. Efficient propagation model can result in proper utilization of economy of mobile industry by providing effective communication and thus increasing number of services per cell. Deterministic modeling is the most considerable solution to the modeling of wireless propagation channel. The main propagation mechanisms considered in radio propagation are diffraction, reflections, and transmission through the obstacles [1]. The diffraction phenomena occur when incident rays hit edges or corners of obstacles in the propagation medium. For the analysis of diffraction phenomena Geometrical theory of diffraction (GTD) and Uniform Theory of diffraction were widely used by researchers. GTD gives acceptable result in illumination region for the prediction of diffracted field but it fails to predict the diffracted field in the shadow region. Pathak formulated diffraction coefficient for curved edge formed by perfectly conducting curved or plane surface [2].

Diffraction coefficient given by Pathak is based on UTD approach, which provide valid result in transition regions adjacent to shadow and reflection boundary. Diffraction coefficient given by Pathak was limited for only perfectly conducting wedges. Luebbers modified the result by multiplying the Fresnel Reflection coefficient to the component of diffraction coefficient such that, diffraction coefficient become workable for lossy dielectric wedges [3]. The heuristic coefficient by Luebbers gives accurate result in the vicinity of the reflection boundary but fails in a deep shadow region. To improve accuracy of Luebbers heuristic coefficient, Holm further modified the original coefficient formulated by luebbers with a multiplication factors to be used in the coefficient [4]. In our work for the calculation of diffracted field and distorted pulse Holms coefficient is used.

All the above diffraction coefficients were proposed for frequency domain and as it is preferable to work directly in time domain. Each and every parameters that can be calculated in UWB system, such as the number of multipath, the delay, the power, and the distortion of every single path are easily evaluated with the help of TD profile. FD solution involves the calculation of channel response for every frequency separately, which is very inefficient for such large bandwidth as in UWB signal. It is rather feasible to work directly in time-domain than to first evaluate the response in frequency domain and then taking its inverse Fourier transform. In the TD approach, a general solution from the impulse response of a resultant path is considered, irrespective of band-width and this resultant impulse response can be convolved with any transmitted signal. The TD coefficients thus can be inserted into the channel, which will thus predict the distortion in the signal.

The time domain uniform geometrical theory of diffraction (UTD) for perfectly conducting wedge was first given by T. W. Veruttipong [7]. This time domain UTD theory was used in various scenarios where single, double and multiple diffraction were involved [8-10]. Pathak also introduced time domain uniform geometrical theory of diffraction for perfectly conducting wedge [11]. This TD solution was obtained by Fourier inversion of the corresponding UTD diffraction coefficient for a perfectly conducting wedge given by Kouyoumjian and Pathak. To calculate received field after double and multiple diffractions, a new approach TD-UTD-PO was discussed in [12-13]. An algorithm has been discussed in [14], to predict the TD diffracted field after an arbitrary number perfectly conducting wedge having different interior angles. This

algorithm is computationally much efficient than the TD-UTD approach for multiple diffraction.

In urban microcellular scenario and indoor scenario especially in non-line of sight (NLOS) communication in deep shadow regions, where the reflected and diffracted field components are weak, transmitted field component proves to be very significant [15]. So it becomes important to analyze the effect of transmitted field through a wall for UWB communication in microcellular and indoor scenario.

The TD solutions for transmission of UWB signals through a dielectric slab were presented in [16, 17]. Here multiple reflections inside the slabs were ignored due to their weak contribution. Another TD solution for transmission through a dielectric slab, considering a limited number of internal reflections, was presented in [18]. The measurements depicting the characterization of different materials within UWB range along with the discussion about dispersion suffered by UWB signals due to penetration through the walls were presented in [19,20]. According to them, in certain cases, the multiple reflections inside the slab decay rapidly. In such cases, the single pass and multiple pass techniques provide the same results. Another work in [21] presented UWB pulse reflections and transmissions through complex wall structures, found in indoor propagation environments, through numerical FDTD simulations. A simplified TD model for transmission of UWB signals through a dielectric slab was presented in [22, 23]. The TD solutions for the reflection and transmission through a dielectric slab incorporating the multiple internal reflections, was presented in [24].

In [25], a TD transmission coefficient for transmission through an interface involving free space and dielectric material has been studied and structures like single wedge and single building scenarios have been analyzed. A FD model was developed in [26] for transmission through multiple layers in the 3-10 GHz band. Though a TD model for UWB signals transmitting through a dielectric slab with interface having free space and dielectric medium exists in literature [27, 21,25]. In our work we have considered the building scenario, in which UWB signals transmitted through the wall of building and then it will arrive at the receiver. We have proposed TD solution for received field calculation after penetration through wall of building.

1.4 Organization of thesis

Chapter 2: The chapter deals with the time domain transmission channel modeling. In this chapter first we have discussed the propagation environment and then ray tracing algorithm has been discussed. Further the expression for transmitted received signal in both frequency and time domain has been discussed.

Chapter 3: The chapter deals with the diffraction channel modeling. The expression for diffracted received signal in both time and frequency domain has been discussed in this chapter.

Chapter 4: It analyzes the results of the simulations & results. The TD results have been validated with the inverse fast Fourier transform (IFFT) of the corresponding exact frequency domain result, and the computational efficiency of TD method is demonstrated against FD domain method.

Chapter 5: This chapter contains the conclusion of the thesis and some suggestions for future work. The reference materials that are used in this thesis directly follow the conclusion and suggestion section.

Chapter 2

Time domain Transmission channel Modeling

In this chapter, Time Domain modeling for transmission of UWB signals through a 3-dimensional building scenario is presented. In radio communication, the main physical phenomena for the propagation of channel are reflection, diffraction and transmission through the building. These are the main phenomena which cause the distortion in the UWB pulse. In radio propagation of UWB signals, especially in non line of sight (NLOS) communication in deep shadow regions, the transmitted field component proves to be very significant. When UWB pulses propagate through channel (free space) distortion occurs. There are two basic approaches to analysis the distortion in UWB pulse. (i) To obtain frequency-domain (FD) solution of the propagation channel and then taking IFFT of the results (ii) Direct time-domain (TD) solution. UWB signal is having a huge bandwidth, so it is more efficient to analysis UWB propagation directly in time domain because in time domain all the frequencies are treated simultaneously. In this chapter we analysis the transmission of UWB signals through building for arbitrary position of transmitter and receiver. Considering the building is made of low loss material, time domain formulation for transmission coefficient for both soft and hard polarization is presented. Time domain formulation for the propagation loss and then for transmitted field at the receiver is also presented. In chapter 4, time domain results have been validated with the inverse fast Fourier transform (IFFT) of the corresponding exact frequency domain result. The computational efficiency of both methods is also compared in chapter4.

2.1 Propagation Environment:

There are two possible cases for the transmission of UWB signals in this building scenario. (i) Transmitter height (h_t) is greater than building height (h_b) i.e. ($h_t > h_b$) and (ii) Transmitter height (h_t) is less than building height (h_b) i.e. ($h_t < h_b$). Fig 2.1 (a) shows the transmission through the 3-D building (with low loss materials) scenario.

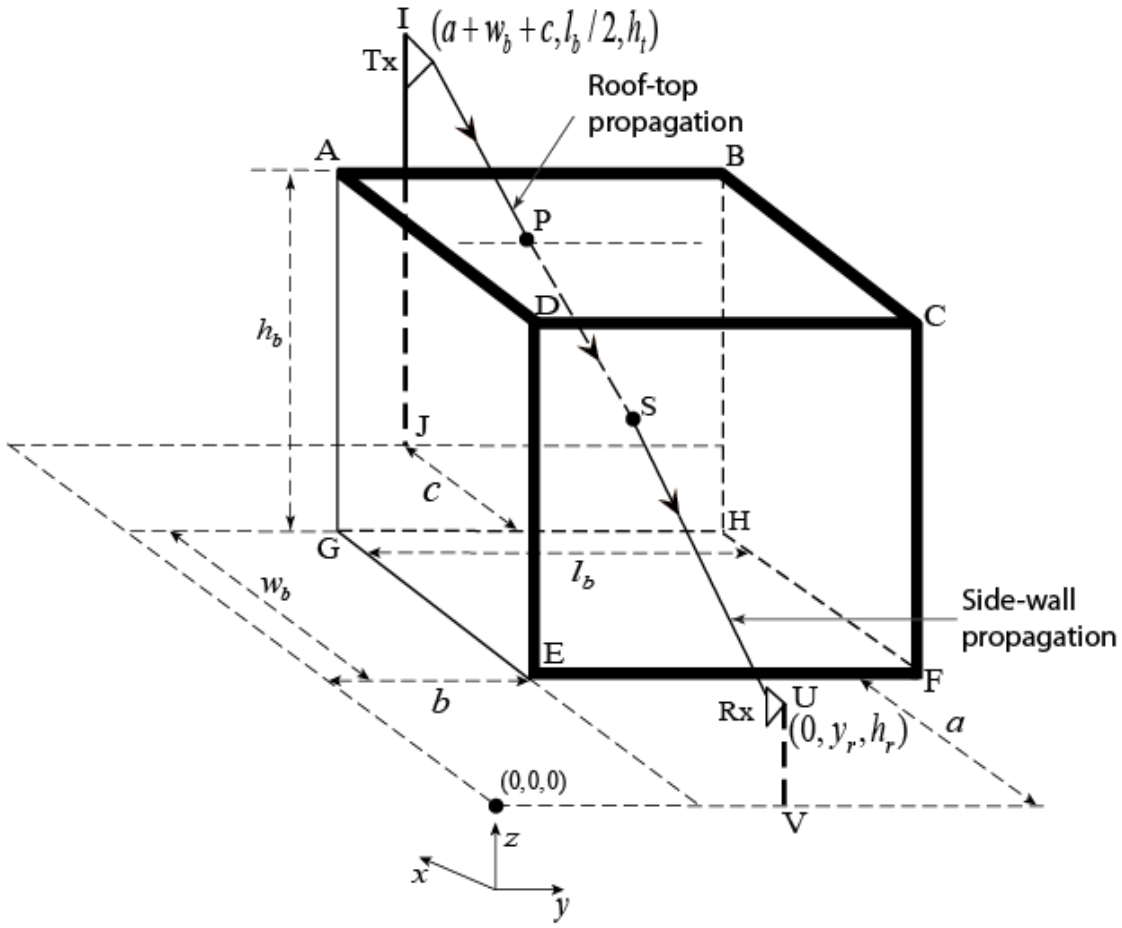

Fig 2.1 (a) Transmission through the 3-D building scenario with $h_t > h_b$

2.1.1 Transmitter height (h_t) is greater than building height (h_b) case

Transmitter (Tx) height h_t is considered greater than building height h_b with l_b as the building length and w_b as the building width. Transmitter is positioned at distance c behind the building and at half length of building (along y-direction). Receiver (Rx) height h_r is lower than building height and its position is fixed along the x and z direction while varying along the y direction. As can seen from Fig 2.1 (a), for $h_t > h_b$, transmission through building comprises roof-top and side wall propagation. Fig 2.1(b) and Fig 2.1 (c) shows front view for roof-top propagation and side view for side-wall propagation respectively with d_1 and d_2 as the width of roof and side-wall respectively. The plane along which the ray propagate from Tx to Rx through the building changes with the movement of Rx along the y direction which result in change in d_2 also.

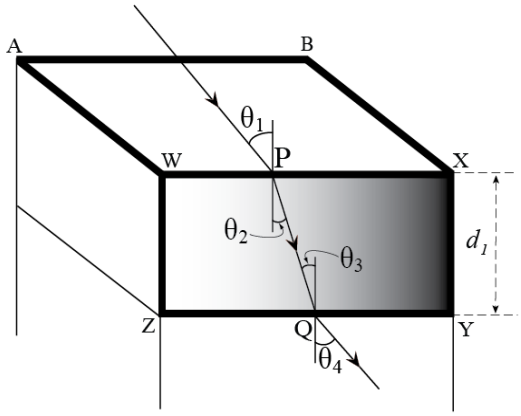

Fig 2.1 (b) Front view for roof-top propagation

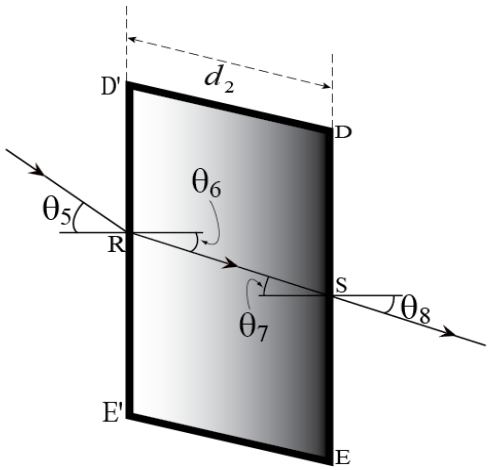

Fig 2.1(c) Side view for side-wall propagation

2.1.2 Transmitter height (h_t) is less than building height (h_b) case

Transmitter (Tx) height h_t is considered less than building height h_b, Receiver (Rx) height h_r is also lower than building height and its position is fixed along the x and z direction while varying along the y direction.

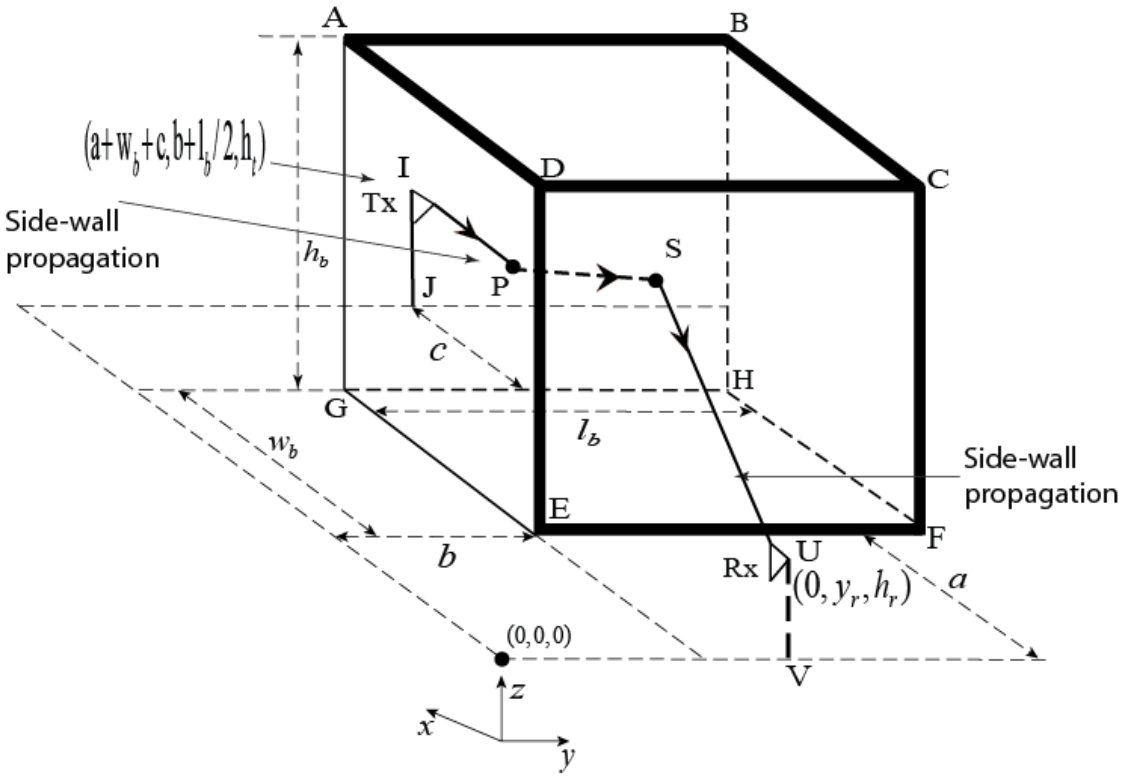

Fig 2.1 (d) Transmission through the 3-D building scenario with $h_t < h_b$

Transmission of UWB signals through building comprises both opposite side wall propagation. The plane along which the ray propagate from Tx to Rx through the building changes with the movement of Rx along the y direction which result in change in width of opposite side wall also.

2.2 Ray Tracing

Ray tracing algorithm is used to determine the path followed by field in wireless propagation environment. The intersection points of ray path at roof-top and side wall of the building (For the case when ($h_t > h_b$) are find out using the parametric form of equation of line [30]. Assume that (x_t, y_t, z_t) and (x_r, y_r, z_r) are the co-ordinates or transmitter and receiver, respectively. The parametric equation for these two points is given as

$$\frac{(x-x_r)}{(x_t-x_r)} = \frac{(y-y_r)}{(y_t-y_r)} = \frac{(z-z_r)}{(z_t-z_r)} = t \qquad (2.1)$$

The Transmitter and Receiver co-ordinates for the case when transmitter height is greater than building height are $(a+w_b+c, b+l_b/2, h_t)$ and $(0, y_r, h_r)$. Hence the parametric equation reduces to

$$\frac{(x)}{(a+w_b+c)} = \frac{(y-y_r)}{(b+l_b/2-y_r)} = \frac{(z-z_r)}{(z_t-h_t)} = t \qquad (2.2)$$

Transmission point on roof-top plane can be obtained by considering the equation of roof-top plane as z = h_b

$$t = \frac{(h_b-h_r)}{(h_r-h_t)}, \qquad x = t*(a+w_b+c),$$

$$y = t*(b+l_b/2-y_r)+y_r, \qquad z = t*(h_t-h_r)+h_r$$

Similarly, the transmission point on the other surface of building can be obtained by using this approach. After finding the transmission point on roof-top plane and side wall we can trace the exact path followed by UWB pulse in this building scenario.

Fig 2.2(a) shows the side view representation of the propagation scenario considered in Fig 2.1 (a). Parameters $r_i(i = 1{:}5)$ are the distances traversed by the transmitted field through the structure from the Tx up to Rx. Angles $\theta_1, \theta_3, \theta_5, \theta_7$ are the incidences angles with $\theta_2,\ \theta_4,\ \theta_6,\ \theta_8$ as the angles of refraction at points 'P', 'Q', 'R', and 'S' respectively. It can be seen from Fig 2.1 (a) and Fig 2.2 (a) that for $h_t > h_b$ transmission through building is the propagation through the corner of the building comprising roof-top and side-wall propagation.

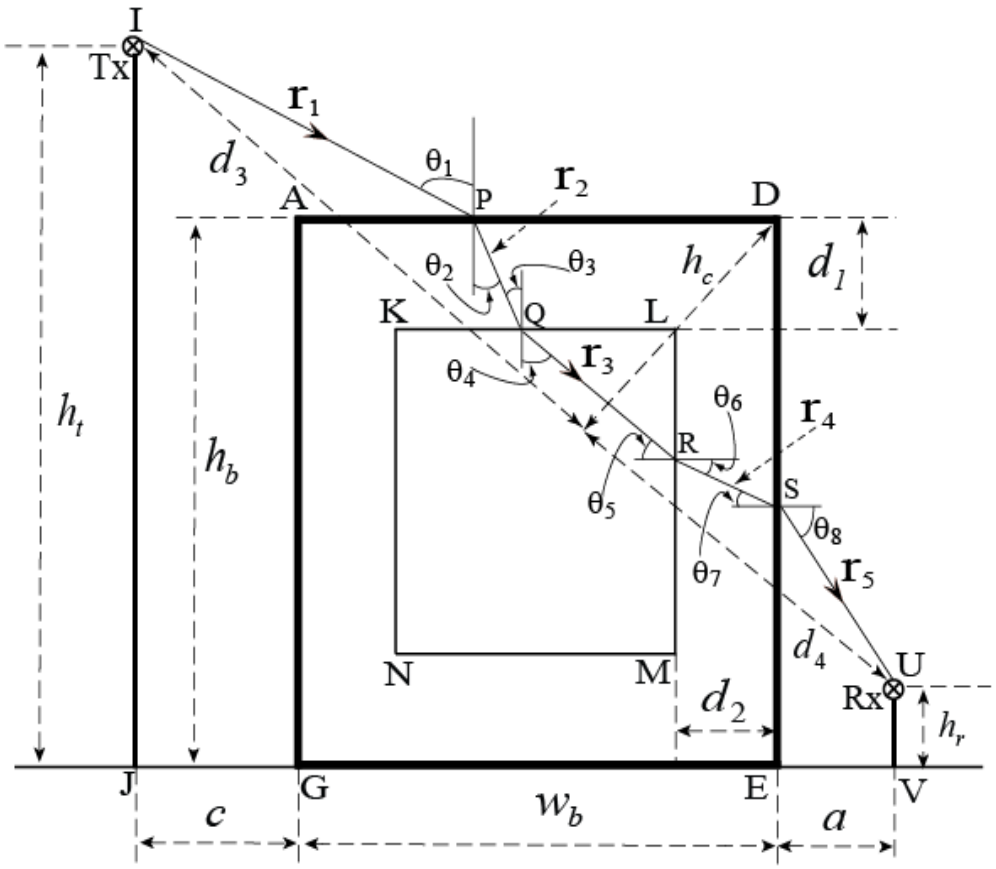

Fig 2.2 (a) Side view for propagation through the 3-D building scenario with $h_t > h_b$

Fig 2.2 (a) shows the error between actual transmitted path (dotted) and ray traced path (solid) for the propagation scenario discussed in Fig. 2.1(a). Fig 2.2 (b) shows the side view representation of transmission through the building for transmitter positioned below the building height. Two opposite side-walls propagation is considered for this kind of scenario. Widths d_1 and d_2 change with Rx movement along y direction.

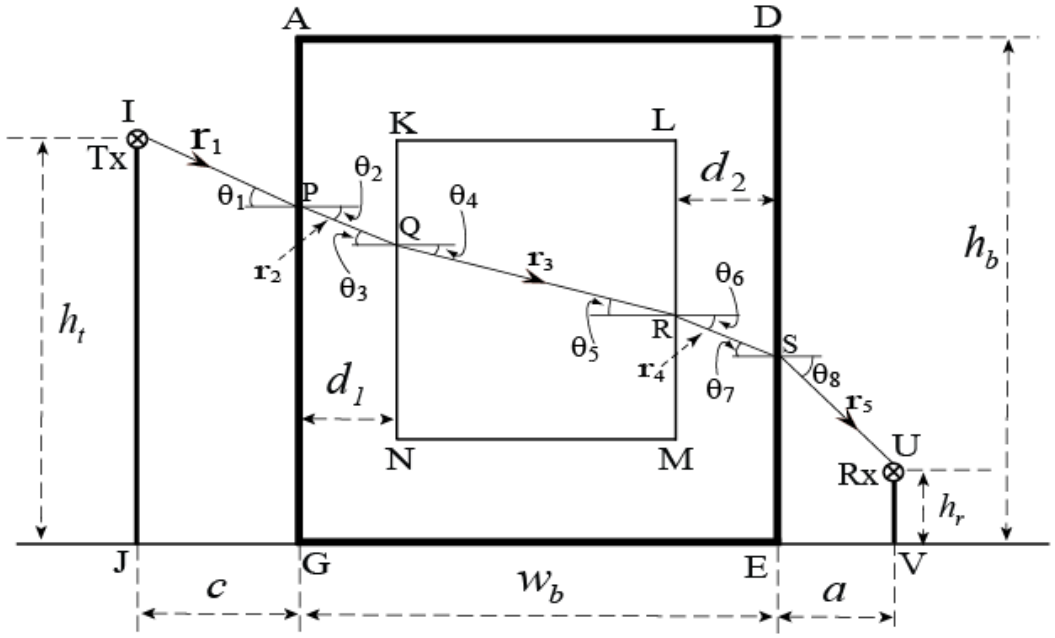

Fig 2.2 (b) Side view for propagation through the 3-D building scenario with $h_t < h_b$

The proposed algorithm to trace the exact path of transmitted field through 3-D building scenario, when transmitter height is greater than building height

- 3-Dimensional problem is converted into 2- Dimensional problem by considering the 3- D scenario as a collection of various 2-Dimensional Tx-Rx planes.

- Consider transmitter is fixed at location with coordinates x=0, y=h_t, where h_t is the height of transmitter. Load the co-ordinates of receiver and all transmission points on roof-top surface and side wall surface of building.

- Considering the roof-top wall of building, choose an arbitrary point with incident angle θ_i of the incident ray from transmitter with respect to normal at the roof-top surface of the building. Compute the incident angles $\theta_3, \theta_5, \theta_7$ on others wall of building and true refracted angles $\theta_2,\ \theta_4,\ \theta_6,\ \theta_8$ as shown in Fig 2.2 (a).

- Compute the co-ordinate of all points P, Q, R, S that lies in the transmitted path on different walls of building.

- Compute the y co-ordinate of the transmitted path at receiver end and let this value be h_{ray}. h_{ray} is the height of estimated ray at the receiver end. The error vector (e_{error}) is defined as difference of h_{ray} and height of receiver h_r. i.e. $e_{error} = h_t - h_r$

- This process is repeated for each sample point of the incident angle on the roof-top wall of building and value of error is stored in error vector (e_{error}).

- Find the minimum error from the vector e_{error}. If this minimum error is less than the desired threshold, then the transmission path corresponding to that error's value is the desired path otherwise the step size $\Delta\theta_i$ is reduced till the minimum error is less than the set threshold error.

By using this ray tracing algorithm, the best appropriate transmitted path can be obtained. The accuracy of this ray tracing algorithm is presented in table 1.

Table 1

Accuracy of proposed ray-tracing algorithm

Step size $\Delta\theta_i$ (in degree)	1	0.6	0.1	0.05	0.001
Min. absolute error, e	54.6×10^{-3}	23.1×10^{-3}	75×10^{-4}	2.67×10^{-4}	4.3×10^{-5}

2.3 FD Transmission Model:

The general expression for the transmitted field (in frequency domain) at the receiver for any polarization is given by [15, 31].

$$E_{RX}(\omega) = \left(\frac{E_i}{r_{total}}\right) T_{total,s,h}(\omega) L_{total,s,h}(\omega) \qquad (2.3)$$

Where, E_i is the relative amplitude of spherical source, r_{total} is the total distance traversed by the transmitted field from Transmitter to Receiver. In this building scenario,

transmitted field path from transmitter to receiver, intersect at four different points on the different walls of building. $T_{total,s,h}(\omega)$ represent the product of all four FD transmission coefficient which occur along a given transmission path between transmitter and receiver. The subscripts 's' and 'h' refer to soft and hard polarization respectively. When transmitted field propagate in free space and also inside the wall (made of different dielectric material) losses occur. $L_{total,s,h}(\omega)$ represent the total propagation path-loss suffered by the transmitted field between transmitter and receiver [28]. Total propagation path-loss include free space propagation loss and losses occur inside wall of building.

In general transmission coefficient for hard and soft polarization is given as [25], [32]

$$T_h(\omega) = 1 + R_h(\omega) = \frac{2\eta_2 \cos\theta_i}{\eta_2 \cos\theta_i + \eta_1 \cos\theta_t} \tag{2.4}$$

$$T_s(\omega) = \left(\frac{\cos\theta_i}{\cos\theta_t}\right)\{1 + R_s(\omega)\} = \frac{2\eta_2 \cos\theta_i}{\eta_2 \cos\theta_t + \eta_1 \cos\theta_i} \tag{2.5}$$

Where θ_i is the angle of incidence, θ_t is the refracted angle, both considered with respect to the normal to the surface of incidence, $R_h(\omega)$ is the Fresnel reflection coefficients for hard polarizations and $R_s(\omega)$ for soft polarization, and η_1 and η_2 are the characteristic impedances of medium-1 and medium-2 respectively(from fig 2.3 (a)). The characteristic impedances of free space is given as $\eta_0 = \sqrt{\mu_0 / \varepsilon_0}$ and for dielectric medium is given as $\eta = \sqrt{\mu / \varepsilon}$, where μ is the permeability and $\tilde{\varepsilon} = \varepsilon + (\sigma / j\omega)$ is the complex permittivity of the medium. Further μ is defined as $\mu = \mu_0 \mu_r$, where μ_0 is the free space permeability and μ_r is the relative permeability of medium. The real part of the complex dielectric permittivity is $\varepsilon = \varepsilon_o \varepsilon_r$, where ε_0 is free space permittivity and ε_r is the relative dielectric permittivity of medium. Attenuation and distortion occur in transmitted signal when it travel in dielectric medium of wall and amount of attenuation and distortion depends on the distance travelled with the dielectric wall of building and its dielectric properties. Fig 2.3 (a) shows the ray propagation in different lossy dielectric medium.

The general expression for propagation constant is given by $\gamma(\omega) = \alpha(\omega) + j\beta(\omega)$ where α is the attenuation constant and β is the phase-shift constant for the given medium.

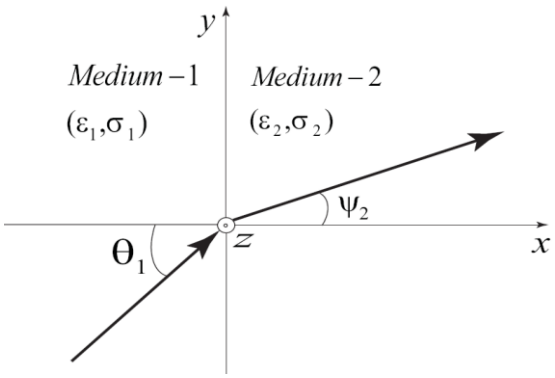

Fig. 2.3 Ray propagation in different lossy dielectric medium.

In a general case, when mediums 1 and 2 are lossy materials (nonzero conductivity which implies $\alpha(\omega) \neq 0$), the refracted angle $\theta_t(\omega)$ is a complex frequency dependent number. By using the Snell's law of refraction [32] the true real refraction angle $\psi_t(\omega)$ can be calculated.

For lossy media, Snell's law of refraction across the interface in Fig. 2.3 (a) can be written as

$$\gamma_1(\omega)\sin\theta_1 = \gamma_2(\omega)\sin\{\theta_2(\omega)\} \tag{2.6}$$

For the geometry of Fig. 2.3 (a),

$$\begin{aligned}\cos\{\theta_2(\omega)\} &= \sqrt{1-\sin^2\{\theta_2(\omega)\}} = \sqrt{1-\sin^2\theta_1[\gamma_1(\omega)/\gamma_2(\omega)]} \\ &= s(\omega)\exp[j\zeta(\omega)] = s(\omega)[\cos\zeta(\omega) + j\sin\zeta(\omega)]\end{aligned} \tag{2.7}$$

Where $\gamma_1(\omega) = j\beta_1(\omega)$ and $\gamma_2(\omega) = \alpha_2(\omega) + j\beta_2(\omega)$

Thus the true refracted angle [32] is given as $\psi_t(\omega) = \tan^{-1}\{t(\omega)/q(\omega)\}$ (2.8)

With $t(\omega) = \beta_1(\omega)\sin\theta_1$ and $q(\omega) = s(\omega)[\alpha_2(\omega)\sin\zeta(\omega) + \beta_2(\omega)\cos\zeta(\omega)]$.

From 2.8 it is clear that the true refraction angle is also frequency dependent in nature, which means that the true real angles of refraction are different for different frequency components of the UWB signal. Thus, a single UWB ray incident on a lossy dielectric material actually splits into a beam of rays after refraction, corresponding to all the frequency components comprising the bandwidth of the signal. It means that the different frequency components of the transmitted signal follow different paths after refraction up to Rx. However, we will show later that for low-loss dielectric obstacles (i.e. $\sigma / w\varepsilon << 1$), for UWB signals, the different true refracted angles reduce to an effective, constant real angle.

So during the TD analysis for low-loss cases we assume the refracted angle to be a constant value to obtain the effective single path travelled by the TD transmitted field as discussed in propagation environment of Fig 2.2 (a). The accuracy of such an assumption is established through the comparison between the obtained TD transmitted field and the actual IFFT-FD transmitted field.

2.4 TD Transmission Model

To obtain the time domain formulation for the transmitted field we can take inverse Laplace transform to the FD formulation, which are obtained after applying the low-loss approximation to the original FD solution. The proposed TD solution is accurate for transmission through low loss dielectric obstacles. In time domain, transmitted field at receiver is given as

$$e_{RX}(t) = \left[e_i(t) / r_{total} \right] * \Gamma_{total,s,h}(t) * l_{total,s,h}(t) \qquad (2.9)$$

with '$*$'representing the convolution operator, $l_{total,s,h}(t)$ [16,17] is the TD counterpart of the term $L_{total,s,h}(\omega)$, $\Gamma_{total,s,h}(t)$ is the TD counterpart of term $T_{total,s,h}(\omega)$ of equation 2.3

2.4.1 Proposed Time Domain Transmission and Reflection Coefficient

In this section we derive the time domain transmission and Reflection coefficients for both hard and soft polarizations. While considering the low loss assumption for dielectric medium, the proposed time domain expression can be used for any kind of obstacles. Relative magnetic permeability is close to one for non magnetic medium (e.g. plywood, drywall).

In our work building is taken as obstacles and it is considered that wall of building is made of low loss dielectric material. If loss tangent value $(\sigma/\omega\varepsilon)$ of dielectric material is very much less than unity then dielectric material is said to have low-loss characteristic. So, in case of low loss dielectric obstacle the true angle of refraction is independent of frequency of entire UWB frequency range.

The approximated angle of refraction is given as

$$\psi_t \simeq \sin^{-1}(\sin\theta_i \ / \sqrt{\varepsilon_r}) \tag{2.10}$$

For the case of hard polarization, transmission coefficient for the wave entering a low-loss dielectric medium from air or free space is given as (from [32])

$$T_{ad,\mathrm{h}}(\omega) = \frac{2\eta\cos\theta_i}{\eta\cos\theta_i + \eta_0\cos\psi_t} \tag{2.11}$$

From (15), we get

$$T_{ad,\mathrm{h}}(\omega) = \frac{2\cos\theta_i}{\cos\theta_i + \left(\sqrt{\frac{\varepsilon_0\varepsilon_r + \sigma/\ j\omega}{\varepsilon_0}}\right)\cos\psi_t} \tag{2.12}$$

After further manipulation and replace $s \to j\omega$

$$T_{ad,\mathrm{h}}(\mathrm{s}) = 1 - \left(\frac{\sqrt{s+\tau} - k_{ad,s}\sqrt{s}}{\sqrt{s+\tau} + k_{ad,s}\sqrt{s}}\right) \tag{2.13}$$

Where $k_{ad,\mathrm{h}} = (\cos\theta_i / \cos\psi_t)(1/\sqrt{\varepsilon_r})$ and $\tau = (\sigma/\varepsilon)$

Now using inverse Laplace technique we get

$$\gamma_{ad,\mathrm{h}}(t) = L^{-1}[\mathrm{T}_{ad,\mathrm{h}}(\mathrm{s})] = \mathrm{L}^{-1}\left[1 - \left(\left\{\frac{\sqrt{s+\tau} - k_{ad,\mathrm{h}}\sqrt{s}}{\sqrt{s+\tau} + k_{ad,\mathrm{h}}\sqrt{s}}\right\}\right)\right] \tag{2.14}$$

Time domain transmission coefficient for soft polarization is given as

$$\gamma_{ad,\mathrm{h}}(t) = \delta(t) - \mathrm{r}_{ad,\mathrm{h}}(t)$$

Where $r_{ad,s}(t)$ is given as

$$r_{ad,\mathrm{h}}(t)=\left[K_{ad,\mathrm{h}}\delta(t)\right]+\frac{4k_{ad,\mathrm{h}}}{\left(1-k_{ad,\mathrm{h}}^2\right)}e^{-pt}\left[\frac{K_{ad,\mathrm{h}}}{2}X_{ad,\mathrm{h}}+\frac{(1-X_{ad,\mathrm{h}})}{(2\mathrm{K}_{ad,\mathrm{h}})}-\frac{(pt)X_{ad,\mathrm{h}}}{4}\right] \quad (2.15)$$

With $K_{ad,\mathrm{h}}=\left(\frac{1-k_{ad,\mathrm{h}}}{1+k_{ad,\mathrm{h}}}\right)$, $X_{ad,\mathrm{h}}=e^{-\left(\frac{K_{ad,\mathrm{h}}pt}{2}\right)}$ and $p=\frac{\sigma}{2\varepsilon}=\frac{\tau}{2}$

Time domain transmission coefficient for soft polarization for the field entering from a low loss dielectric medium into free space (air) can be derived from (2.4) and [32]

$$T_{da,\mathrm{h}}(\omega)=\frac{2\eta_0\cos\theta_i}{\eta_0\cos\theta_i+\eta\cos\psi_t}$$

$$T_{da,\mathrm{h}}(\omega)=\frac{2\cos\theta_i\left(\sqrt{1+\frac{\sigma}{s\varepsilon}}\right)\sqrt{\varepsilon_r}}{\cos\theta_i\sqrt{\varepsilon_r}+\left(\sqrt{1+\left(\frac{\sigma}{s\varepsilon}\right)}\right)\cos\psi_t} \quad (2.16)$$

After manipulation $$T_{da,\mathrm{h}}(\mathrm{s})=1+\left(\frac{\sqrt{s+\tau}-k_{da,\mathrm{h}}\sqrt{s}}{\sqrt{s+\tau}+k_{da,\mathrm{h}}\sqrt{s}}\right) \quad (2.17)$$

$$\gamma_{da,\mathrm{h}}(t)=L^{-1}[\mathrm{T}_{da,\mathrm{h}}(\mathrm{s})]=\mathrm{L}^{-1}\left[1-\left(\left\{\frac{\sqrt{s+\tau}-k_{da,\mathrm{h}}\sqrt{s}}{\sqrt{s+\tau}+k_{da,\mathrm{h}}\sqrt{s}}\right\}\right)\right] \quad (2.18)$$

Where $K_{da,\mathrm{h}}=\left(\cos\psi_t/\cos\theta_t\right)(1/\sqrt{\varepsilon_r})$ and expression for TD soft transmission coefficient for this case is given as

$$\gamma_{da,\mathrm{h}}(t)=\delta(t)+\mathrm{r}_{da,\mathrm{h}}(t) \quad (2.19)$$

Where

$$r_{da,\mathrm{h}}(t)=\left[K_{da,\mathrm{h}}\delta(t)\right]+\frac{4k_{da,\mathrm{h}}}{\left(1-k_{da,\mathrm{h}}^2\right)}e^{-pt}\left[\frac{K_{da,\mathrm{h}}}{2}X_{\mathrm{da,h}}+\frac{(1-X_{da,\mathrm{h}})}{(2\mathrm{K}_{da,\mathrm{h}})}-\frac{(pt)X_{da,\mathrm{h}}}{4}\right] \quad (2.20)$$

With $X_{da,\mathrm{h}}=e^{-\left(\frac{K_{da,\mathrm{h}}pt}{2}\right)}$, $K_{da,\mathrm{h}}=\left(\cos\psi_t/\cos\theta_t\right)(1/\sqrt{\varepsilon_r})$

Generalized time domain transmission coefficient for hard polarization is obtained as

$$\gamma_h(t) = \left[\delta(t) + r_h(t)\right] \tag{2.21}$$

Where $r_s(t)$ is the time domain counterpart of $r_s(\omega)$.Now For the two cases of propagation discussed above, corresponding TD reflection coefficient are ' $-r_{ad,\mathrm{h}}(\mathrm{t})$ ' and $r_{da,\mathrm{h}}(\mathrm{t})$ respectively. Similarly TD transmission coefficient expression for soft polarization wave, propagating from air to low loss dielectric medium is given as

$$T_{ad,\mathrm{s}}(\omega) = \frac{2\eta\cos\theta_i}{\eta\cos\psi_t + \eta_0\cos\theta_i} \tag{2.22}$$

After manipulation we obtained as

$$\gamma_{ad,\mathrm{s}}(t) = L^{-1}[\mathrm{T}_{ad,\mathrm{h}}(\mathrm{s})] = \mathrm{L}^{-1}\left[1-\left(\left\{\frac{\sqrt{s+\tau}-k_{ad,\mathrm{s}}\sqrt{s}}{\sqrt{s+\tau}+k_{ad,\mathrm{s}}\sqrt{s}}\right\}\right)\right]\left(\frac{\cos\theta_i}{\cos\psi_t}\right) \tag{2.23}$$

Where $k_{ad,\mathrm{s}} = (\cos\psi_t / \cos\theta_i)(1/\sqrt{\varepsilon_r})$

After solving we get $$\gamma_{ad,\mathrm{h}}(t) = \left[\delta(t) - \mathrm{r}_{ad,\mathrm{h}}(t)\right]\left(\frac{\cos\theta_i}{\cos\gamma_t}\right) \tag{2.24}$$

Where $r_{ad,\mathrm{s}}(t) = \left[K_{ad,\mathrm{s}}\delta(t)\right] + \frac{4k_{ad,s}}{\left(1-k_{ad,s}^2\right)}e^{-pt}\left[\frac{K_{ad,s}}{2}X_{ad,s} + \frac{(1-X_{ad,s})}{(2\mathrm{K}_{ad,s})} - \frac{(pt)X_{ad,s}}{4}\right]$

And $K_{ad,\mathrm{s}} = \left(\frac{1-k_{ad,\mathrm{s}}}{1+k_{ad,\mathrm{s}}}\right)$, $X_{ad,\mathrm{s}} = e^{-\left(\frac{K_{ad,s}pt}{2}\right)}$

Now for the case when soft polarized wave propagating from dielectric medium to air

$$\gamma_{da,\mathrm{h}}(t) = \left[\delta(t) + \mathrm{r}_{da,\mathrm{h}}(t)\right]\left(\frac{\cos\theta_i}{\cos\psi_t}\right) \tag{2.25}$$

$$r_{da,\mathrm{s}}(t) = \left[K_{da,\mathrm{s}}\delta(t)\right] + \frac{4k_{da,\mathrm{s}}}{\left(1-k_{da,\mathrm{s}}^2\right)}e^{-pt}\left[\frac{K_{da,\mathrm{s}}}{2}X_{\mathrm{da,s}} + \frac{(1-X_{da,\mathrm{s}})}{(2\mathrm{K}_{da,\mathrm{s}})} - \frac{(pt)X_{da,\mathrm{s}}}{4}\right] \tag{2.26}$$

Where $K_{da,\mathrm{s}} = \left(\frac{1-k_{da,\mathrm{s}}}{1+k_{da,\mathrm{s}}}\right)$, $k_{ad,\mathrm{s}} = (\cos\psi_t / \cos\theta_i)(1/\sqrt{\varepsilon_r})$ and $X_{da,\mathrm{s}} = e^{-\left(\frac{K_{da,s}pt}{2}\right)}$

Generalized time domain transmission coefficient for soft polarization is obtained as

$$\gamma_s(t) = \left[\delta(t) + r_s(t)\right]\left(\frac{\cos\theta_i}{\cos\psi_t}\right) \tag{2.27}$$

Where $r_s(t)$ is the time domain counterpart of $r_s(\omega)$.Now For the two cases of propagation discussed above, corresponding TD reflection coefficient are ' $-r_{ad,s}(t)$ ' and $r_{da,s}(t)$ respectively.

2.4.2 Transmitted field through building Profile

The expression for transmitted field through building profile in frequency domain is given as

$$E_{RX}(\omega) = \left(E_i(\omega)/r_{total}(\omega)\right)\left(\prod_{m=1}^{4} T_{m,s,h}(\omega)\right)\left(\exp(-j\beta_0 r_1)\exp(-\alpha_b\, r_3)\prod_{n=2}^{5}\exp\left\{-\left(\alpha_{en}(\omega) + j\beta_{en}(\omega)\right)\right\}\right) \tag{2.28}$$

Where α_b is specific attenuation constant for interior interior of building and it depends on the internal architecture of the building. By using the low-loss approximation we get a single effective transmitted path through building (See Fig 2.2 (a)). The approximate transmitted field through building is given as

$$E_{RX}(\omega) \simeq \left(\frac{E_i(\omega)}{r_{total}}\right)\left(T_{1,s,h}(\omega)T_{2,s,h}(\omega)T_{3,s,h}(\omega)T_{4,s,h}(\omega)\right)L_{total,s,h}(\omega) \tag{2.29}$$

Where $T_{1,s,h}(\omega)$, $T_{2,s,h}(\omega)$, $T_{3,s,h}(\omega)$, $T_{4,s,h}(\omega)$ are the FD Transmission coefficient with respect to points 'P', 'Q', 'R', 'S' (From Fig 2.2(a) and 2.2(b)). r_{total} is the total distance travelled by the field from Tx to Rx. Applying low loss approximation the approximate FD pat-loss for this building scenario is given as

$$L_{total,s,h}(\omega) \simeq \exp\left[-j\omega d\sqrt{\mu\varepsilon}\left(1+\frac{\sigma}{2j\omega\varepsilon}\right)\left(\sqrt{\frac{\varepsilon_r}{\varepsilon_r-\sin^2\theta_1}}+\sqrt{\frac{\varepsilon_r}{\varepsilon_r-\sin^2\theta_5}}\right)\right]\exp\left(-j\beta_0(r_1+r_5)\right)\exp(-\alpha_b\, r_3) \tag{2.30}$$

Where r_3 is the distance travelled by field in interior of building and $r_1 + r_5$ is the distance travelled by the field in the free space from Tx to Rx.

Now the Time Domain transmitted field for considered building scenario is given by

$$e_{RX}(t) \simeq \left(\frac{e_i(t)}{r_{total}} \right) * \Gamma_{1,s,h}(t) * \Gamma_{2,s,h}(t) * \Gamma_{3,s,h}(t) * \Gamma_{4,s,h}(t) * l_{total,s,h}(t) \tag{2.31}$$

Where $\Gamma_{1,s,h}(t) * \Gamma_{2,s,h}(t) * \Gamma_{3,s,h}(t) * \Gamma_{4,s,h}(t) = \Gamma_{total,s,h}(t)$ with $\Gamma_{1,s,h}, \Gamma_{2,s,h}, \Gamma_{3,s,h}, \Gamma_{4,s,h}$ as the TD expressions for the transmission coefficients at points 'P', 'Q', 'R' and 'S' in Fig. 2.2(a) and Fig 2.2(b) .

The term $l_{total,s,h}(t)$ represents the TD propagation path loss corresponding to FD path loss expression given in (35). The expression for $l_{total,s,h}(t)$ is given as

$$\begin{aligned} l_{total,s,h}(\mathrm{t}) \simeq \exp\left\{ \left(-(\sigma d)/2\right) \sqrt{\frac{\mu_2}{\varepsilon_2}} \left(\sqrt{\frac{\varepsilon_r}{\varepsilon_r - \sin^2\theta_1}} + \sqrt{\frac{\varepsilon_r}{\varepsilon_r - \sin^2\theta_5}} \right) \right\} * \delta\left(t - \frac{r_1 + r_5}{c} \right) \\ * \delta\left\{ t - \sqrt{\mu_1 \varepsilon_1} \left(d_1 \sqrt{\frac{\varepsilon_r}{\varepsilon_{r1} - \sin^2\theta_1}} + d_2 \sqrt{\frac{\varepsilon_r}{\varepsilon_r - \sin^2\theta_5}} \right) \right\} \exp(-\alpha_b \, \mathrm{r}_3) \end{aligned} \tag{2.32}$$

Chapter 3

Time Domain Diffraction channel modeling

In this chapter, time domain channel modeling for diffraction of UWB signals for a 3- D building scenario is presented. When incident field hit edges of the building walls, Diffracted fields are produced. This diffraction phenomenon plays an important role when there is no LOS path between transmitter and receiver. In this chapter we analysis the diffraction of UWB signals through building for arbitrary position of transmitter and receiver. Time domain formulation for diffraction coefficient for both hard and soft polarization is presented. The expression for Diffracted field at receiver is also presented in both frequency and time domain. In next chapter, these time domain results have been validated with the inverse fast Fourier transform (IFFT) of the corresponding exact frequency domain results. The computational efficiency of both methods is also compared in next chapter.

3.1 Diffraction Coefficient

To calculate the effect of diffraction various methods has been discussed in Literature. The generalized geometrical properties of diffraction are described by the angle ϕ' for the incoming ray, and by ϕ for the diffracted ray, both with respect to the 0-face as shown in Fig 3.1

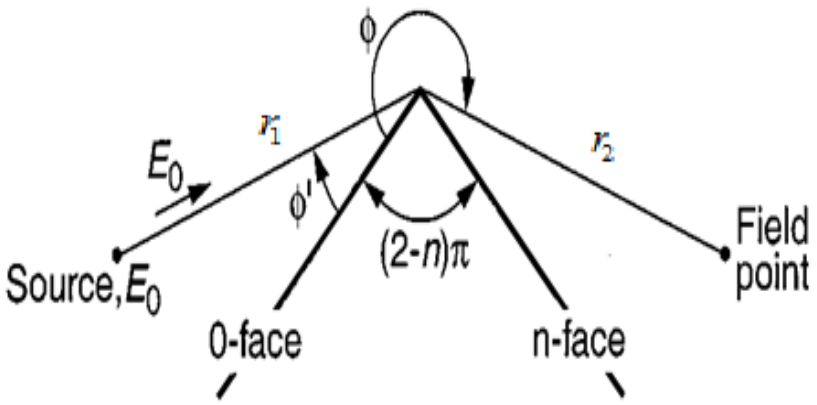

Fig 3.1 Geometry for diffraction for wedge case

Angle ϕ' represents the angle of incidence and it is defined as the angle formed by the ray joining the transmitter and the vertex of the wedge, and 0-face of the wedge. Angle ϕ represents the angle of diffraction and it is defined as the angle of the ray joining the receiver and the vertex of the wedge with respect to 0-face of the wedge. n is defined as the wedge index and exterior angle is considered as $n\pi$, So the wedge angle will be equal to $(2-n)\pi$. So the value of n entirely depends on the value of the wedge angle considered.

In our case we have considered the building scenario, and for the building profile internal wedge angle is $\frac{\pi}{2}$. Wedge index for building case can be calculated as:

$$(2-n)\pi = \frac{\pi}{2} \qquad \text{So, } n = \frac{3}{2}$$

3.1.1 Pathak Diffraction Coefficient

Pathak has given the UTD diffraction coefficient which gave accurate result for the perfectly conducting wedges [2]. Pathak's diffraction coefficient can be defined as:

$$D_{s,h}(\phi,\phi') = \left[D1 + D2 \mp \{D3 + D4\} \right] \tag{3.1}$$

Where,

$$D_1 = \frac{-\exp[-j(\pi/4)]}{2n\sqrt{2\pi k}} \times \left[\cot\left(\frac{\pi + (\phi - \phi')}{2n} \right) F\left[kLa^{+}(\phi - \phi') \right] \right]$$

$$D_2 = \frac{-\exp[-j(\pi/4)]}{2n\sqrt{2\pi k}} \times \left[\cot\left(\frac{\pi - (\phi - \phi')}{2n} \right) F\left[kLa^{-}(\phi - \phi') \right] \right]$$

$$D_3 = \frac{-\exp[-j(\pi/4)]}{2n\sqrt{2\pi k}} \times \left[\cot\left(\frac{\pi - (\phi + \phi')}{2n} \right) F\left[kLa^{-}(\phi + \phi') \right] \right]$$

$$D_4 = \frac{-\exp[-j(\pi/4)]}{2n\sqrt{2\pi k}} \times \left[\cot\left(\frac{\pi + (\phi + \phi')}{2n} \right) F\left[kLa^{+}(\phi + \phi') \right] \right]$$

Negative sign in D is used for soft polarization while positive sign is used for hard polarization. L is the distance parameter, n is wedge index and $F(x)$ is the Fresnel transition function:

$$F(x) = 2j\sqrt{x}e^{jx}\int_{\sqrt{x}}^{\infty} e^{-j\tau^2}d\tau$$

$$L = \frac{R_1 R_2}{R_1 + R_2}$$

The $a^{\pm}$ function used in calculation of the diffraction coefficient is defined as:

$$a^{\pm}(\beta) = 2\cos^2\left[\frac{2n\pi N^{\pm} - \beta}{2}\right]$$

In which $N^{\pm}$ are the integers which most nearly satisfy the equations:

$2n\pi N^{+} - (\beta) = \pi$ and $2n\pi N^{-}(\beta) = -\pi$ with $\beta = \phi \pm \phi'$

3.1.2 Holm's Diffraction Coefficient

Diffraction coefficient given by Pathak is applicable for only perfectly conducting wedges. Holm modified the Pathak's diffraction coefficient in order to make it workable for lossy wedges [4]. The Holm's diffraction coefficient is given as:

$$D^{s,h} = R_0^{s,h}R_n^{s,h}D_1 + D_2 + R_0^{s,h}(\alpha_0)D_3 + R_n^{s,h}(\alpha_n)D_4 \qquad (3.2)$$

Where D_i is the UTD diffraction coefficients where $i = 1:5$, which can be defined in frequency domain as

$$D_i(\omega) = \frac{-\exp(-\mathrm{j}\pi/4)}{2n\sqrt{2\pi k}}\cot(\mathrm{a}_i)\,\mathrm{F}[2\,\mathrm{kLn}^2\sin^2(\mathrm{a}_i)] \qquad (3.3)$$

Where a_i can be defined as $a_1 = [\pi + (\phi - \phi')]/(2\mathrm{n})$,

$a_2 = [\pi - (\phi - \phi')]/(2\mathrm{n})$, $a_3 = [\pi - (\phi + \phi')]/(2\mathrm{n})$ and $a_4 = [\pi + (\phi + \phi')]/(2\mathrm{n})$

R_0 and R_n are the Fresnel reflection coefficient corresponding to 0-face and n-face respectively [33]. Subscripts 's' and 'h' represent soft and hard polarization respectively. The Fresnel reflection coefficient for a finitely conducting surface having a relative dielectric constant ε_r is defined as

$$R^h(\phi) = \frac{\cos(\phi) - \sqrt{\in_r - \sin^2(\phi)}}{\cos(\phi) + \sqrt{\in_r - \sin^2(\phi)}} \qquad (3.4)$$

And $$R^s(\phi) = \frac{\in_r \cos(\phi) - \sqrt{\in_r - \sin^2(\phi)}}{\in_r \cos(\phi) + \sqrt{\in_r - \sin^2(\phi)}} \quad (3.5)$$

Where $\in_r = \in_r - j\frac{\sigma}{\omega \in_0}$ is the wedge complex relative permittivity. The angle argument ϕ for 0-case equal to $\phi = \phi'$ and for n case it will be $\phi = n\pi - \phi'$.

3.2 Propagation Environment:

There are various possible paths through which the transmitted signal arrives at receiver after diffraction at edges of the building's wall. We will discuss the two major paths, along which the signal arrive at receiver.

(i) Single diffraction.

(ii) Single diffraction followed by ground reflection.

Propagation environment for these cases are discussed as:

3.2.1 Single Diffraction

Fig 3.2 shows the Single diffraction at the edge of building, edge is formed by the front wall and top-roof wall of building.

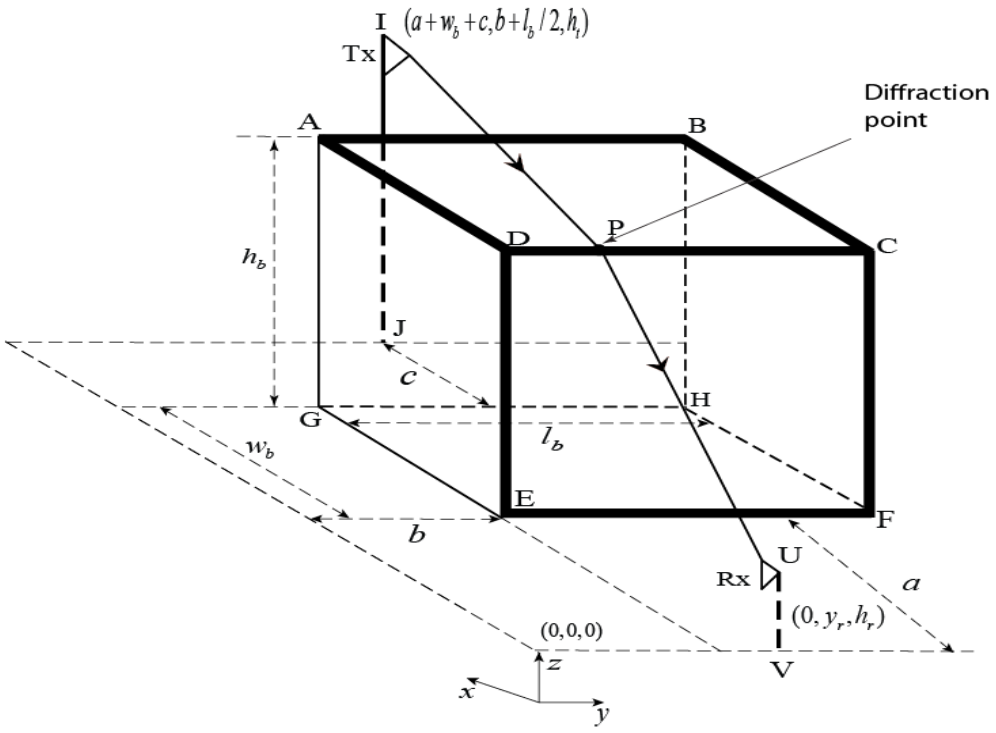

Fig 3.2 Single diffraction in 3-D building scenario

Transmitter (Tx) height h_t is considered greater than building height h_b and it is positioned at distance c behind the building and at half length of building (along y-direction). Receiver (Rx) height h_r is lower than building height and its position is fixed along the x and z direction while varying along the y direction. l_b and w_b are length of building and width of building respectively. The plane along which the ray propagate from Tx to Rx changes with the movement of Rx along the y direction. Fig 3.3 shows the side view representation of the propagation scenario considered in Fig 3.2 for a fixed position of receiver in y direction. Three dimensional problem is converted into 2-dimensional problem by considering a plane through which ray propagate, for a fixed position of receiver in y direction and all the diffraction parameters are calculated along the considered plane.

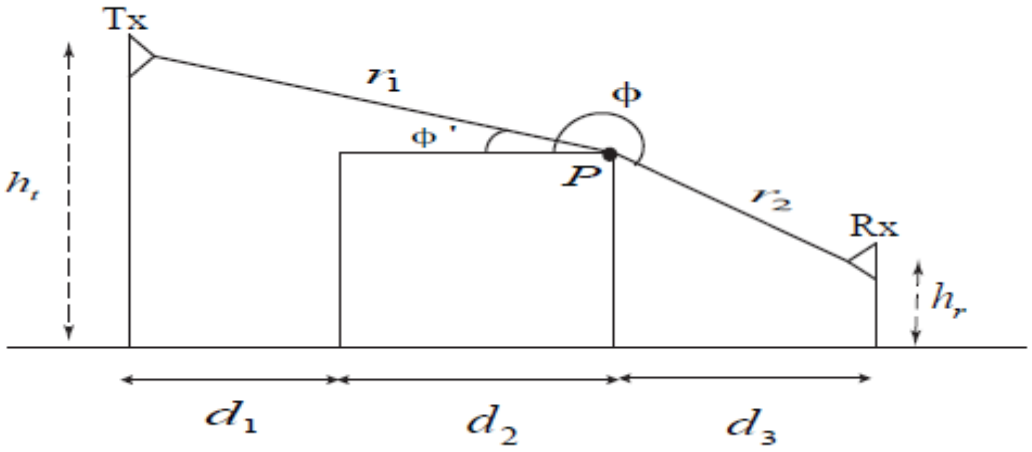

Fig 3.3 Side view representation for single diffraction scenario

Where r_1 is the distance from the transmitter to diffraction point 'P', r_2 is the distance from diffraction point 'P' to receiver. ϕ' and ϕ are the angle of incident and angle of diffraction respectively. d_1 is the distance from transmitter to back wall of building , d_2 is the width of building and d_3 is distance from point 'P' to receiver along the considered plane.

Various components of Fig 3.3 can be calculated as

$$r_1 = \sqrt{(h_t - h_b)^2 + (d_1 + d_2)^2}$$

$$r_2 = \sqrt{(h_b - h_r)^2 + (d_3)^2}$$

Incident angle $\phi' = \tan^{-1}\left(\frac{h_t - h_b}{d_1 + d_2}\right)$

Diffracted angle $\phi = 3\frac{\pi}{2} - \tan^{-1}\left(\frac{d_3}{h_b - h_r}\right)$

The expression for the diffracted field at receiver in frequency domain is given as

$$E_R(\omega) = \left(\frac{E_i(\omega)}{r_1}\right) D^{s,h}(\omega) A_1(r_1) \exp(-jk(r_1 + r_2)) \quad (3.6)$$

Where $D^{s,h}(\omega)$ is the holm's diffraction coefficient which has been discussed earlier, $E_R(\omega)$ is the field at receiver, $E_i(\omega)$ is the transmitted field, k is the wave number and it is equal to $k = \frac{\omega}{c}$, c is the speed of light. $A_1(r_1)$ is the spreading factor which can be given as $A_1(r_1) = \sqrt{r_1 / (r_1(r_1 + r_2))}$.

3.2.2 Single diffraction followed by the ground reflection:

In this case there will be diffraction at edge of building's wall followed by reflection at ground, as shown in fig. 3.4 below.

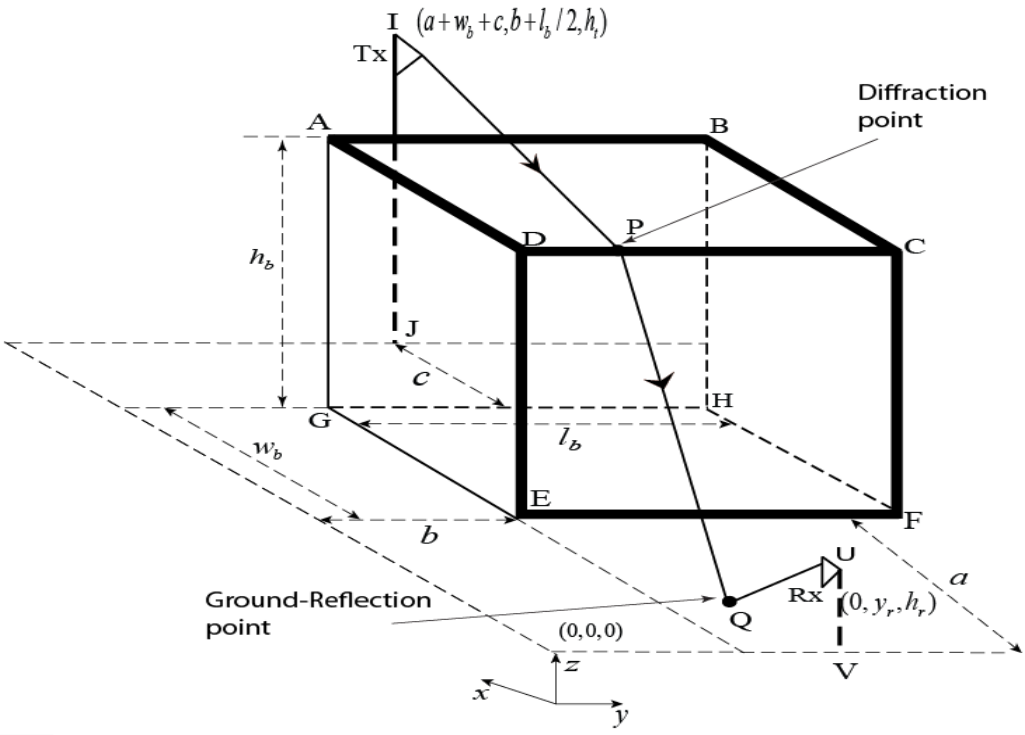

Fig 3.4 Single diffraction followed by the ground reflection for 3-D building scenario

Position of Tx and Rx and the method of converting the 3-D problem into 2-D is same as discussed in case (i). Fig 3.5 shows the side view representation of the propagation scenario considered in this section, for a fixed position of receiver in y direction. All parameters are calculated according to Fig. 3.5. Where r_1 is the distance from the transmitter to diffraction point 'P', r_2 is the distance from diffraction point 'P' to ground reflection point 'Q', and r_3 is distance from reflection point to the receiver. ϕ' and ϕ are the angle of incident and angle of diffraction respectively. d_1 is the horizontal distance from transmitter to back wall of building, d_2 is the width of building and d_3 is horizontal distance from point 'P' to receiver along the considered plane.

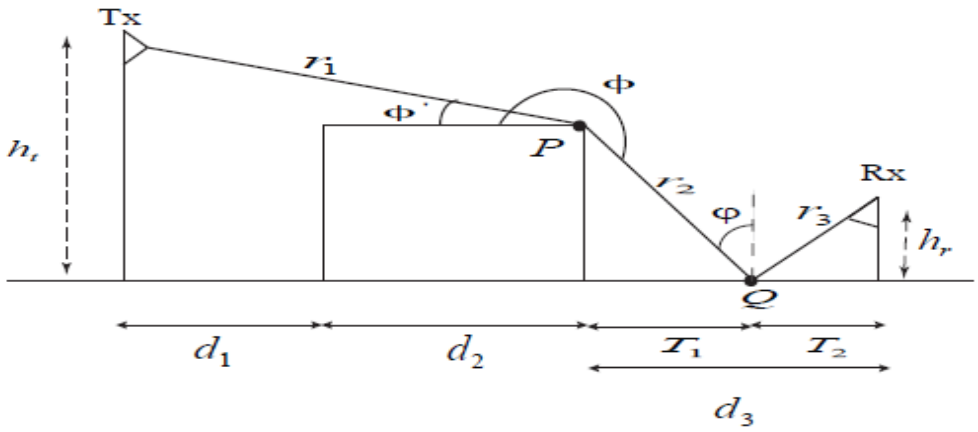

Fig 3.5 Side view representation for single diffraction followed by ground reflection Scenario

Various components of Fig 3.5 can be calculated as

$$r_1 = \sqrt{(h_t - h_b)^2 + (d_1 + d_2)^2}$$

$$\phi' = \tan^{-1}\left(\frac{h_t - h_b}{d_1 + d_2}\right)$$

$$\phi = \pi + \tan^{-1}\left(\frac{h_b}{T_1}\right)$$

By using Snell's law, we can say

$T_2 \tan^{-1}\left(\frac{h_b}{T_1}\right) = \tan^{-1}\left(\frac{h_r}{T_2}\right)$ and $T_2 = d_3 - T_1$

So, T_1 can be given as $T_1 = \left(\frac{h_b d_3}{h_b + h_r}\right)$

The expression for the diffracted followed by reflected field at receiver in frequency domain is given as

$$E_R(\omega) = \left(\frac{E_i(\omega)}{r_1}\right) D(\omega)\, \mathrm{A}_1(r_1) R_Q(\omega) \exp(-\mathrm{jk}(\mathrm{r}_1 + \mathrm{r}_2 + \mathrm{r}_3)) \qquad (3.7)$$

Where spreading factor $A_1(\mathrm{r}_1) = \sqrt{\frac{r_1}{(\mathrm{r}_2 + \mathrm{r}_3)(\mathrm{r}_1 + \mathrm{r}_2 + \mathrm{r}_3)}}$, R_Q is the ground reflection coefficient at point Q. φ is the angle of reflection, calculated with respect to normal to earth surface.

$D(\omega)$ is the diffraction coefficient which has been discussed above.

The approximated reflection coefficient can be given as

$$R_Q(\varphi, \mathrm{s}) = \pm \frac{\sqrt{s+\tau} - k\sqrt{s}}{\sqrt{s+\tau} + k\sqrt{s}} \qquad (3.8)$$

where $k = \beta$ for soft polarization and $k = (\varepsilon_r \beta)^{-1}$ for hard polarization. The + sign is used for soft polarized wave and – sign is used for hard polarized wave. The value of β can be given as

$\beta = \sqrt{\varepsilon_r - \cos^2 \varphi} / \varepsilon_r \sin \varphi$.

3.3 Time domain Analysis

3.3.1 Time domain Diffraction Coefficient

To obtain the time domain expression for diffraction coefficient we can take the inverse Laplace transform of frequency domain holm's diffraction coefficient (equation 3.2). TD holm's diffraction coefficient for non-perfectly conducting building can be given as:

$$d^{s,h}(t) = r_0^{s,\mathrm{h}}(t) * \mathrm{r}_n^{s,h}(t) * d_1(t) + d_2(t) + r_0^{s,h}(t) * d_3(t) + r_n^{s,h}(\mathrm{t}) * \mathrm{d}_4(\mathrm{t}) \qquad (3.9)$$

Where $d_i(t)$ can be given as

$$d_i(t) = -\frac{Ln}{2\pi\sqrt{2c}} \frac{\sin(2a_i)}{\sqrt{t}(t+\gamma_i)} \quad \text{Where i = 1:4.} \tag{3.10}$$

$a_1 = [\pi + (\phi - \phi')]/(2\text{n})$, $a_2 = [\pi - (\phi - \phi')]/(2\text{n})$,

$a_3 = [\pi - (\phi + \phi')]/(2\text{n})$ and $a_4 = [\pi + (\phi + \phi')]/(2\text{n})$

and $\gamma_i = \frac{2Ln^2 \sin^2(a_i)}{c}$

Where '*' denotes the convolution operator. $r_0^{s,h}(t)$ and $r_n^{s,h}(t)$ are the time domain reflection coefficient with respect to 0-face and n-face of building respectively [33]. Here 's' and 'h' denote the soft and hard polarization, the time domain reflection coefficient can be given as:

$$r(t) \approx \pm\left[K\delta(t) + \frac{4k}{(1-k^2)} e^{-at} \left[\frac{K}{2} X + \frac{1}{2K}(1-X) - \frac{at}{4} X \right] \right] \tag{3.11}$$

where, $X = e^{-\frac{Kat}{2}}$ and $a = \frac{\tau}{2}$ where $\tau = \frac{\sigma}{\in_r}$

The leading 'plus' sign is for the soft polarization and 'minus' sign is used for the hard polarization.

For soft polarization, $k = \beta$

For hard polarization, $k = (\in_r \beta)^{-1}$

$$\beta = \frac{\sqrt{\in_r - \sin^2(\theta_i)}}{\in_r \cos(\theta_i)}$$

and $K = \frac{1-k}{1+k}$

When $t \to 0$, then $\frac{1}{\sqrt{t}} \to \infty$, thus $d_i(t)$ approaches to infinity in equation 3.10, there is a singularity in impulse response at t = 0. This singularity causes problems in the numerical calculation [34]. Actually, it is this singular point (at t = 0) that makes the main contribution to the waveform distortion.

This singularity cannot be directly removed by using time-window, if tried so considerable information will be lost. We then integrate the $d_i(t)$, i.e. $\int_0^t d_i(t)$. This integrity removes the singularity condition and we can convolve the signal with incident pulse. Lately, differentiation can be applied to achieve the same result.

3.3.2 Time Domain Diffracted Field for different propagation environment

In this section the expression for the diffracted field at receiver for different propagation environment are formulated.

- **Time Domain Single Diffracted Field**

The TD expression for the diffracted signal at Rx for the propagation environment discussed as in case (i) can be given as

$$E_R(t) = A_1(r_1)\left[\left(\frac{E_i(t)}{r_1}\right) * \mathrm{d}^{s,h}(t)\right] * \delta(\mathrm{t}-(\mathrm{r}_1+\mathrm{r}_2)/\mathrm{c}) \qquad (3.12)$$

Where asterisk '*' denote the convolution and $\delta(\mathrm{t}-(\mathrm{r}_1+\mathrm{r}_2)/\mathrm{c})$ represent the time shift which is equal to the time that the signal need to be traverse the path. $d^{s,h}(t)$ is the time domain diffraction coefficient which has been discussed.

- **Time domain Single diffracted followed by ground reflected field**

In this propagation scenario the transmitted UWB signal diffracted at building corner first, then it is reflected by ground surface before reaching to receiver. To calculate the field at receiver the transmitted signal $E_i(t)$ is convolved with the time domain diffraction coefficient $d(t)$, and the result will be convolved with the TD reflection coefficient $r(t)$. The term $d(t)$ and $r(t)$ has been discussed in previous section (see 3.3.1). The TD field at receiver for this propagation environment can be expressed as

$$E_R(t) = A_1(r_1)\left[\left(\frac{E_i(t)}{r_1}\right) * \mathrm{d}^{s,h}(t)\right] * \delta(\mathrm{t}-(\mathrm{r}_1+\mathrm{r}_2+\mathrm{r}_3)/\mathrm{c}) \qquad (3.13)$$

Where $\delta(\mathrm{t}-(\mathrm{r}_1+\mathrm{r}_2+\mathrm{r}_3)/\mathrm{c})$ represent the time shift which is equal to the time that the signal need to be traverse the path.

Chapter 4

SIMULATION & RESULTS

In this section numerical simulation results of transmitted and diffracted field for all propagation environments are presented. In case of FD analysis of transmission of UWB signal through building, first the frequency components contributing to total transmitted field at receiver are distinguished. As we have discussed earlier (chapter 2) that different frequency components of the transmitted signal follow different paths after refraction up to Rx. So frequency components reaching within an error of 10^{-6} m with respect to receiver are considered as reaching exactly at receiver. Considering only these frequency components the transmitted field at receiver is calculated. To obtain the reference transmitted field, the IFFT of this result is also computed. In TD analysis, by using a ray tracing algorithm (see section 2.3 of chapter 2) based on low loss approximation, a single effective path of the transmitted field through building is traced. The transmitted field along that effective path is calculated in TD. For validation of the proposed solution, The TD transmitted filed results are compared with reference IFFT-FD results. Fig 4.1 shows the Gaussian doublet pulse. In all results the Gaussian doublet pulse is used as the excitation UWB signal.

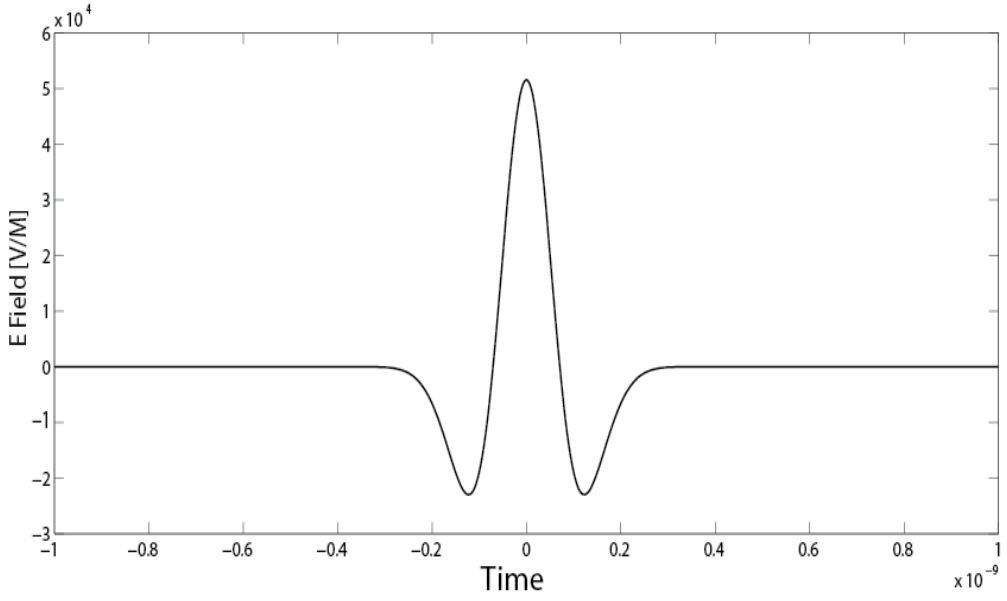

Fig 4.1 Gaussian doublet Pulse

The expression of UWB signals in time domain can be given as

$$s(t) = \left(\frac{1}{\tau}\right)\left(\sqrt{\frac{\tau}{3\sqrt{\pi/2}}}\right)\left(1-\frac{2t^2}{\tau^2}\right)\exp\left(-\frac{t^2}{\tau^2}\right) \tag{4.1}$$

Where τ is the full width half maximum pulse duration with a value of 0.1 ns.

The Fourier transform of $s(t)$ is given as

$$S(f) = 2\times\sqrt{\pi}\times\sqrt{\frac{\tau}{3\sqrt{\pi/2}}}\times\left(\pi^2\tau^2 f^2\right)\times e^{-\pi^2\tau^2 f^2} \tag{4.2}$$

We have considered that obstacle (i.e. building) made up of low loss dielectric materials with relative magnetic permeability as unity and relative dielectric permittivity and conductivity are chosen such that the resulting loss tangent values are in accordance with that of dry-wall, dry-concrete and dry brick (see Table 2). Table 2 shows the electromagnetic properties of the considered materials.

Table 2 Electromagnetic properties of different dielectric materials

Material	Relative Permittivity (ε_r)	Conductivity σ(S/m)
Glass [20]	6.7	0.001
Dry Concrete [28]	5	0.016
Brick [24]	4.4	0.018
Wood [28]	2	0.01

4.1 Time Domain Approximation of Transmitted Field

For the case when Tx height is greater than building height, transmission through building comprises roof-top and side wall propagation and when Tx height is less than building height then transmission through building comprises both opposite side wall propagation. Fig 4.2 and Fig 4.3 shows transmitted field at Rx for these propagation scenario (see Fig 2.1 Fig 2.4 in chapter 2) with different Rx positions, for both soft and hard polarizations. The presented results also show the simulated effective transmission path and the simulated propagation profile in their inset along with the transmitted field.

For both cases height of building and receiver is considered to be equal to be equal to 4m and 1m respectively. The Building's wall is considered to be made of dry concrete having dielectric relative permittivity $\in_r = 5$ and conductivity $\sigma = 0.016$ S/m. In Fig 4.2, height of transmitter is considered to be equal to 6m.

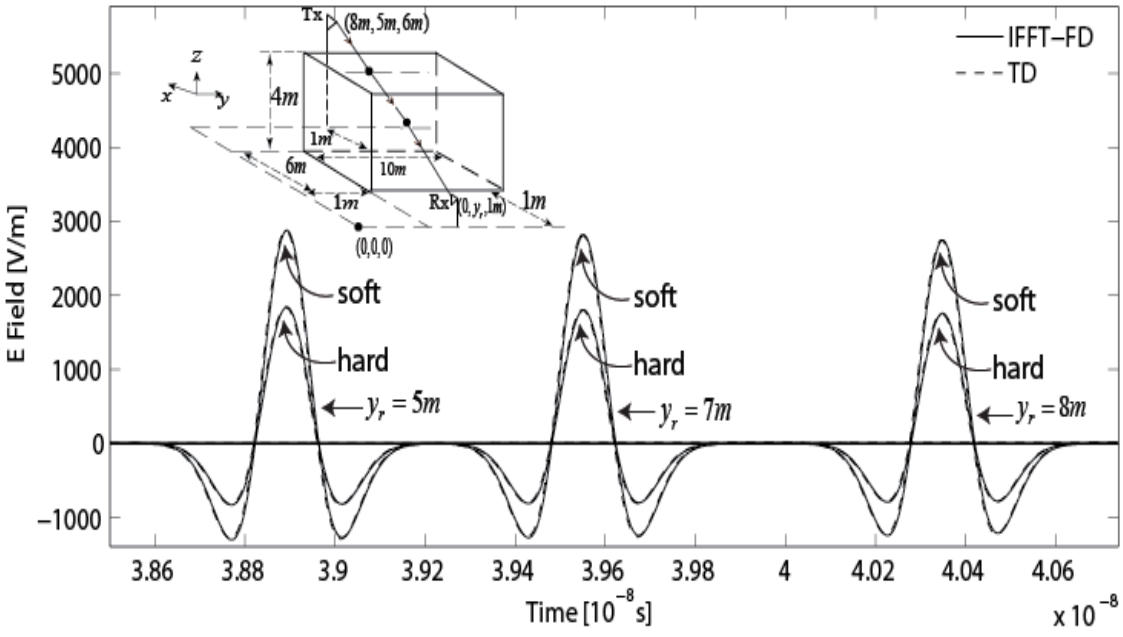

Fig 4.2 Transmitted field through the building structure (for $h_t > h_b$), with dry concrete.

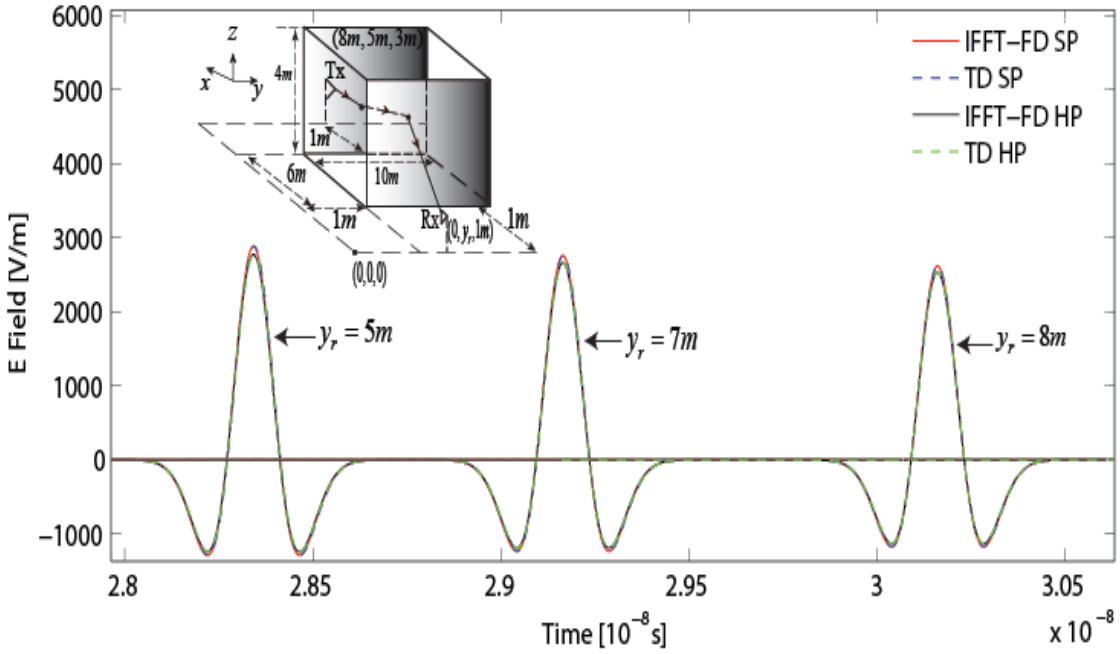

Fig 4.3 Transmitted field through the building structure (for $h_t < h_b$), with dry concrete.

In Fig 4.3, the height of transmitter is considered to be equal to 3m. As it can be seen, the transmitted field at Rx suffers no distortion in shape in comparison to the shape of the excited UWB pulse. The transmitted field is undistorted due to very small magnitude of the loss tangent with respect to unity. However, the amplitude of the transmitted field is attenuated because of the transmission loss through the dielectric mediums. The TD results for transmitted field for both the polarizations are in excellent agreement with corresponding IFFT of exact FD results, thus providing validation to the proposed TD solution. Considering all propagation environments discussed above, if conductivity of the building's wall becomes zero, then the transmitted field computed through IFFT approach is supposed to exactly match the transmitted field computed through TD approach. But in MATLAB simulation, it is observed that some offset value in time-axis still remains between TD and IFFT-FD results and that was noted due to MATLAB limitations. In all the following results, this offset has been compensated.

Fig. 4.4 shows transmitted field at Rx for the case when transmitter height is greater than building height with building structure made up of different dielectric materials, for soft polarization. The TD results are in good agreement with the IFFT-FD results. It is observed that TD and IFFT-FD results match better with decrease in loss tangent, thus validating our low-loss assumption.

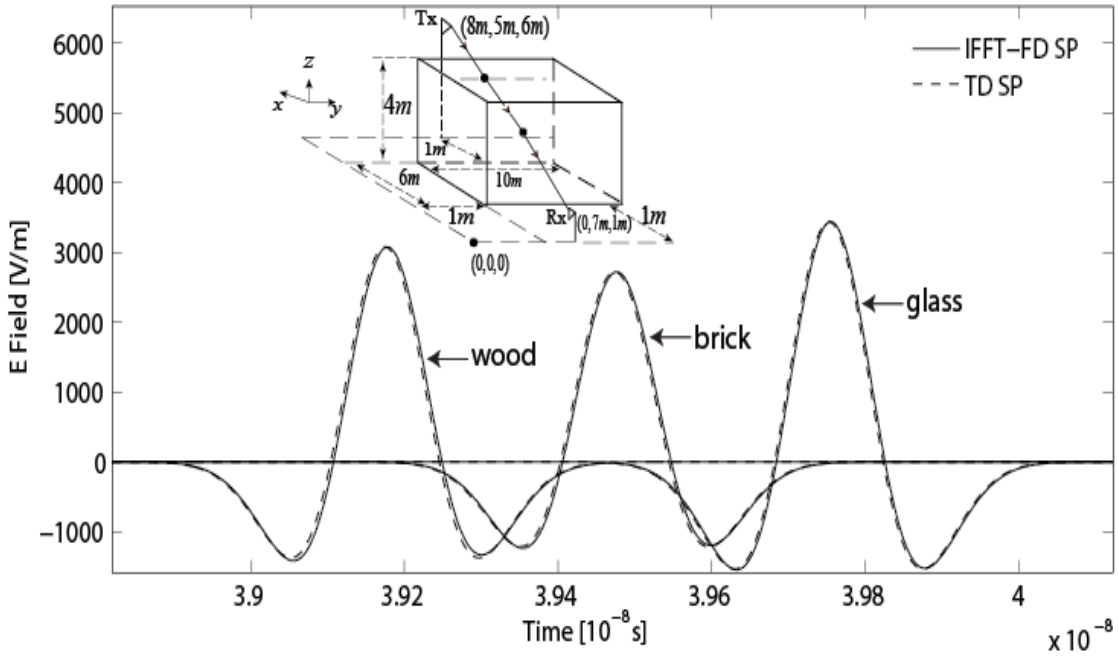

Fig 4.4 Transmitted field through the building structure (for Fig. 2), with glass brick and wood.

Fig 4.5 shows the transmitted field at the receiver for different thickness of building's walls with different receiver position, for both soft and hard polarizations. Other dimensions such as building height, receiver height and transmitter height are taken to be same as that of Fig 4.2. As the transmitter height is greater than building height, transmission of UWB signal comprises the roof-top and side wall propagation. It can be inferred that the transmitted field for hard and soft polarization come closer to each other as the thickness of building's wall increases. Also TD results match closely with the IFFT-FD results.

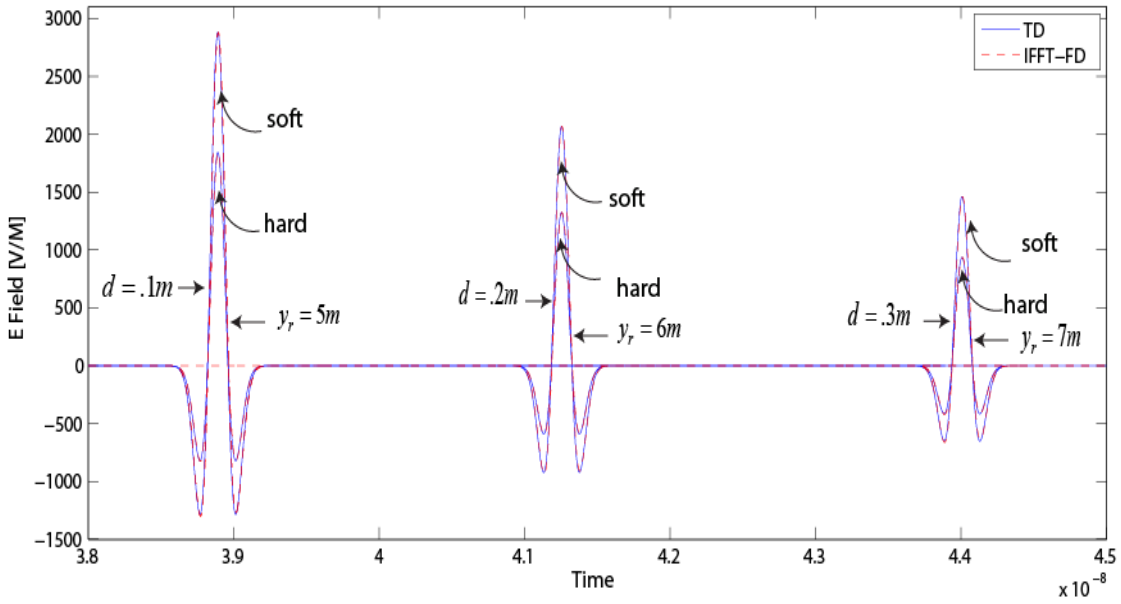

Fig 4.5 Comparison of transmitted field through the building wall of different thickness

4.2 Time Domain Approximation of Diffracted Field

For the case of diffraction we have considered that Tx height is greater than building height. There are two possible ray paths between Tx and Rx, through which an UWB signal can reaches to receiver. (i) In first case the UWB signal get diffracted at building corner and then reaches at receiver end. (ii) In second case, the UWB signal gets diffracted at corner of building and then it is reflected by the ground surface before reaching to receiver.

Fig 4.4 and Fig 4.5 show the received UWB pulse for these propagation scenarios with different receiver position, for both soft and hard polarization. Receiver is moving along

y-direction, diffracted field is calculated when receiver is positioned at 3m and 6m apart from origin in y-direction. The presented results also show the simulated effective diffraction path and the simulated propagation profile in their inset along with the diffracted field.

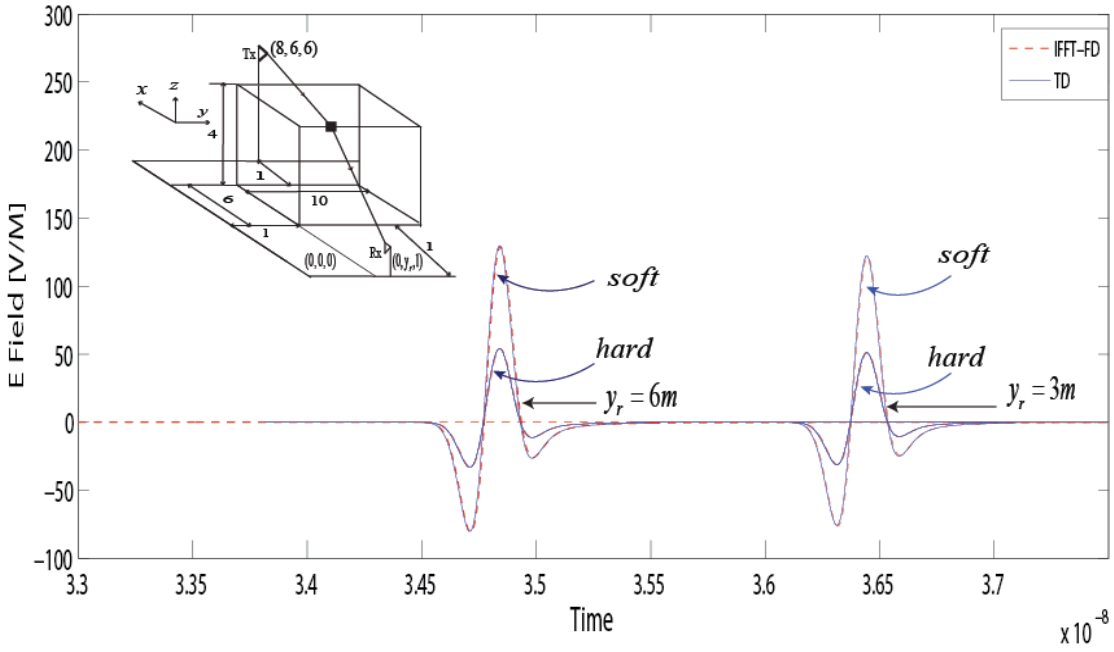

Fig 4.6 Diffracted field by the building structure (for $h_t > h_b$), with dry concrete

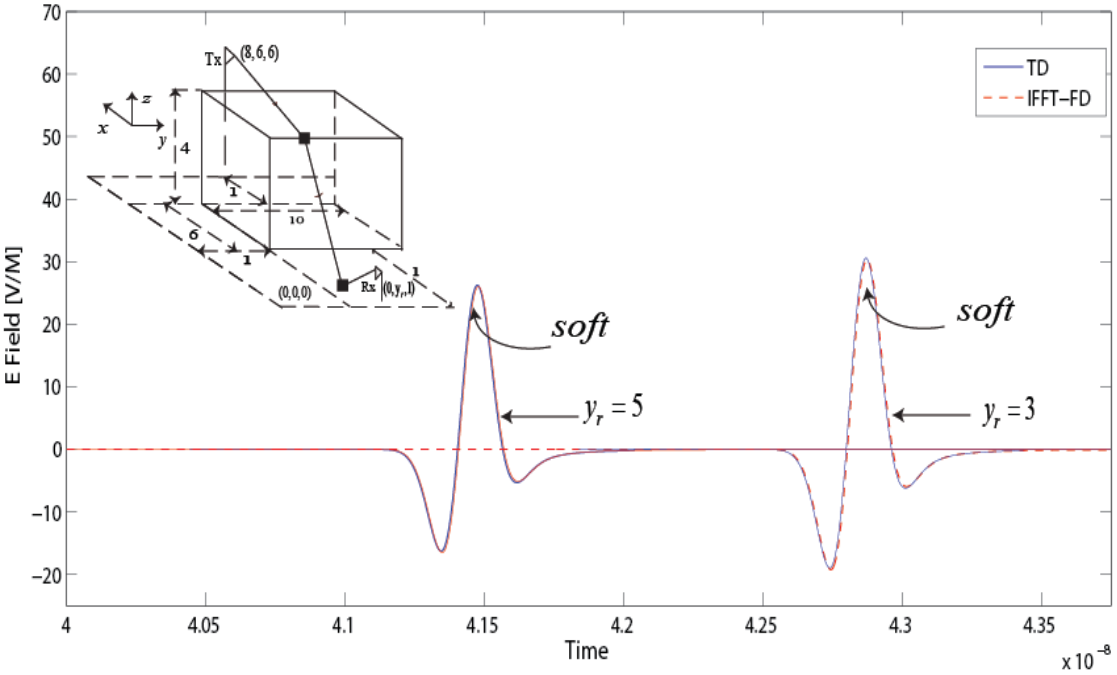

Fig 4.7 Diffracted followed by ground reflected field by the building structure (for $h_t > h_b$), with dry concrete.

It can be seen that the diffracted field at Rx suffers distortion in shape in comparison to shape of excited UWB pulse. The TD results for diffracted field for both the polarizations are in excellent agreement with corresponding IFFT of exact FD results, thus providing validation to the proposed TD solution.

4.3 Comparison of Transmitted and Diffracted Field

In wireless channel the transmitted UWB signal reaches up to receiver by more than one path, resulting in a phenomenon called multipath propagation. The received signal is a distorted version of transmitted signal which degrades the performance of communication system. In this section we compare the received signal from the different paths in multipath environment. The position of receiver is fixed at 5 m apart from origin in y-direction. The height of transmitter, receiver, and building is considered to be equal to 6m, 1m, and 4m respectively. The Building's wall is considered to be made of dry concrete having dielectric relative permittivity $\in_r = 5$ and conductivity $\sigma = 0.016$ S/m. Fig 4.8 shows that single diffracted field and diffracted followed by ground reflected field are highly attenuated and distortion is also more for the same case. But transmitted field at Rx suffers no distortion in shape in comparison to the shape of the excited UWB pulse and attenuation is also very less.

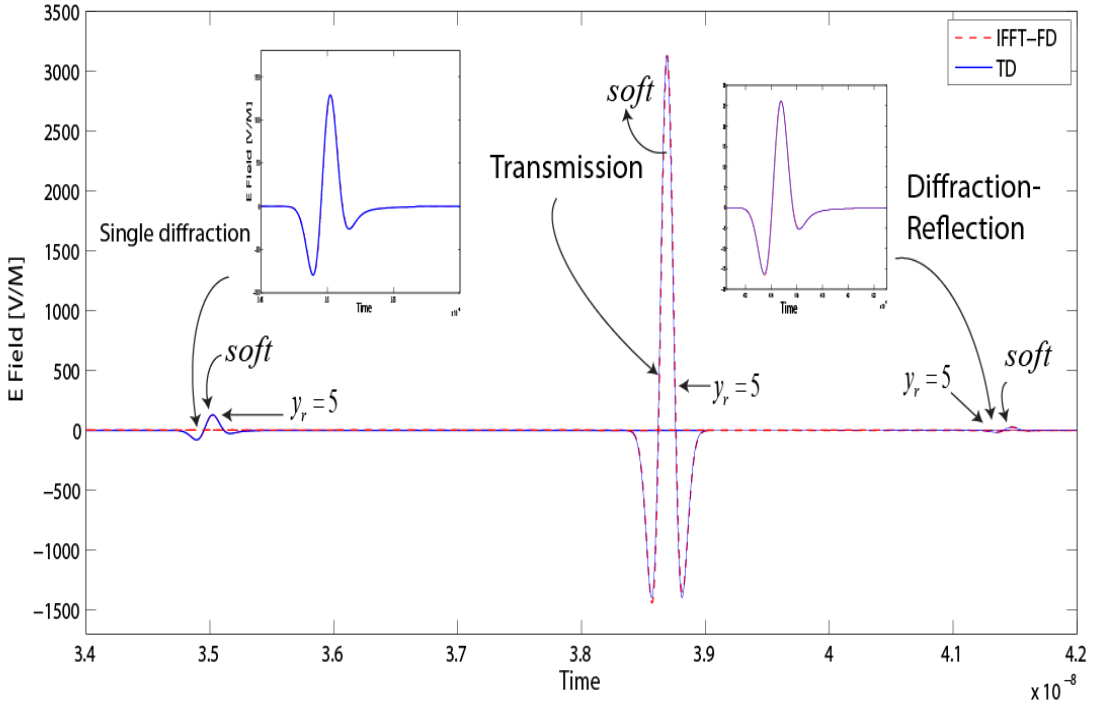

Fig 4.8 Comparison of received signal in multipath environment

From Fig 4.8 it is clear that transmitted field component is very significant in radio propagation of UWB signals, especially in non line of sight (NLOS) communication in deep shadow regions.

4.4 Performance Evaluation of Proposed TD Method

A comparison between the computational times of the IFFT-FD method and the proposed TD solution for different scenarios is presented in Table 3 which establishes that the proposed TD analysis is computationally very efficient in comparison to the IFFT-FD solution. The two main reasons for such a significant reduction in the computational time in TD are:

(i) In proposed TD method for low loss dielectric case, we approximated the multiple transmission paths as in case of FD by a single effective path. (ii) An efficient convolution technique is used in TD method, in which few time samples sufficient to provide accurate result.

Table 3 Average ratios of the computation time of the two methods

Propagation Profile	$T_{IFFT-FD} / T_{TD}$
Building 3-D roof-top and side-wall propagation	~165
Building 3-D side wall propagation	~315

Table 4 shows the variation of normalized mean error and mean square error with increasing loss tangent for all the considered transmission scenarios in this work. It can be concluded from this table that the proposed TD solution performs better for low loss tangent values.

Table 4 Error variation with loss tangent

Los Tangent		0.01918	0.2452	.03997	0.08269	0.13114	0.1712	0.18732
Build-ing $h_t > h_b$	Mean error	$1.388E^{-3}$	$1.642E^{-3}$	$3.244E^{-3}$	$6.612E^{-3}$	$1.465E^{-2}$	$2.54E^{-2}$	$2.712E^{-2}$

Los Tangent		0.01918	0.2452	0.03997	0.08269	0.13114	0.1712	0.18732
Build-ing $h_t > h_b$	Mean Square error	$3.877E^{-5}$	$5.561E^{-5}$	$2.256E^{-4}$	$8.547E^{-4}$	$3.694E^{-3}$	$1.027E^{-2}$	$1.391E^{-2}$
Build-ing $h_t < h_b$	Mean error	$7.507E^{-4}$	$6.308E^{-4}$	$2.121E^{-4}$	$5.269E^{-4}$	$1.931E^{-3}$	$4.029E^{-3}$	$5.383E^{-3}$
	Mean Square error	$1.154E^{-5}$	$8.158E^{-6}$	$7.595E^{-7}$	$3.878E^{-6}$	$5.032E^{-5}$	$2.376E^{-4}$	$4.582E^{-4}$

Chapter 5

CONCLUSION AND FUTURE SCOPE OF WORK

An analytical TD solution has been presented for the transmitted and diffracted field through the 3-D building structure made up of low-loss dielectric materials. Novel ray tracing algorithm for transmission of UWB signal through building is presented with error of an order of 10^{-5}.An analytical TD transmission coefficients are derived for transmission of UWB signal through an interface between air and a low loss dielectric material. The comprehensive FD analysis of diffraction of spherical waves by building structure in microcellular scenario is presented and corresponding TD formulation has been done. The results of the proposed TD solution are validated against the corresponding IFFT-FD results and computational efficiency of both methods is compared. The proposed TD solution outperforms the IFFT-FD analysis in terms of the computational complexity and efficiency. The proposed TD solutions are supposed to be vital in the analysis of UWB communication as they provide a fast and accurate prediction of the total diffracted and transmitted field in microcellular and indoor propagation scenarios.

The TD solution for Slope diffraction can be produced for the prediction of diffracted field through building structure for the future work. Because when height of transmitter is less than building height than slope diffracted field become very significant for radio path loss computation.

REFERENCES

1. A. Karousos, C. Tzaras, "Multiple time domain diffraction for UWB signals," *IEEE Trans. Antennas Propag.*, Vol. 56, 1420-1427, 2008.
2. R. G. Kouyoumjian, P. H. Pathak, "A uniform geometrical theory of diffraction for an edge in a perfectly conducting surface," *Proc. IEEE*, Vol. 62, 1448-1461, 1974.
3. R. J. Luebbers, "A Heuristic UTD Slope Diffraction Coefficient for Rough Lossy Wedges," *IEEE Trans. Antennas Propag.*, Vol. 37, 206-211, 1989.
4. P. D. Holm, A New Heuristic UTD Diffraction Coefficient for Nonperfectly Conducting Wedges," *IEEE Trans. Antennas Propag.*, Vol. 48, 1211-1219, 2000.
5. F. Nekoogar, *Ultra-wideband communications: fundamentals and applications*, Prentice Hall, 2005.
6. Homayoun Nikookar, Ramjee Prasad,"*Introduction to Ultra Wideband Communication for Wireless Communication*" Springer ScienceþBusiness Media B.V. 2009
7. T. W. Veruttipong, "Time-Domain Version of the Uniform GTD," *IEEE.Trans. Antennas Propag.*," vol. 38, 1757–1764, 1990.
8. R. C. Qiu and C. Zhou, "Pulse Distortion Caused by Cylinder Diffraction and its Impact on UWB Communications," *IEEE Trans. Veh. Technol.*," vol. 56, 2385–2391, 2007.
9. F. Capolino and M. Albani, "Time-Domain Double Diffraction at a Pair of Coplanar Skew Edges," *IEEE Trans. Antennas Propag.*," vol. 53, 1455–1469, 2005.
10. P. Górniak and W. Banduriski, "Direct Time-Domain Analysis of an UWB Pulse Distortion by Convex Objects with the Slope Diffraction Included," *IEEE Trans. Antennas Propag.*, vol. 56, 3036–3044, 2008.
11. P. Górniak and W. Banduriski, "Direct Time-Domain Analysis of an UWB Pulse Distortion by Convex Objects with the Slope Diffraction Included," *IEEE Trans. Antennas Propag.*, vol. 56, 3036–3044, 2008.
12. P. Liu and Y. Long, "Time-Domain UTD-PO Solution for Multiple Building Diffraction for UWB Signals," *Electronics Letters*, Vol. 45, 924-926, 2009.

13. T. Han and Y. Long, “Time-Domain UTD-PO Analysis of a UWB Pulse Distortion by Multiple Building Diffraction,” *IEEE Antennas and Wireless Propagation Letters*, Vol. 9, 795-798, 2010.
14. P. Liu, J. Guo, J. Liu, J. Wang, and Y. Long, “Multiple Time-Domain Diffraction of Plane Waves by an Array of Perfectly Conducting Wedges for UWB signals,” *978-1-4244-5708-3/10 2010 IEEE,* 1173-1176, 2010.
15. S. Soni, A, Bhattacharya, “An analytical characterization of transmission through a building for deterministic propagation modeling,” *Microw Opt Technol Lett*, Vol. 53, 1875-1879, 2011.
16. Z. Chen, R. Yao, and Z. Guo, “The Characteristics of UWB Signal Transmitting through a Lossy Dielectric Slab,” *IEEE 60th Veh. Technol.Conf. (VTC2004-Fall)*, vol. 1, 134–138, 2004.
17. R. Yao, Z. Chen, and Z. Guo, “An Efficient Multipath Channel Model for UWB Home Networking,” *0-7803-8451-2/04, IEEE*, 511-516, 2004.
18. R. C. Qiu, “A Generalized Time Domain Multipath Channel and Its Application in Ultra-Wideband (UWB) Wireless Optimal Receiver Design—Part II: Physics-Based System Analysis,” *IEEE Trans. on Wireless Communications*, Vol. 3, 2312-2324, 2004.
19. A. Muqaibel, A. Safaai-Jazi, A. Bayram, A.M. Attiya and S.M. Riad, “Ultra wideband through-the-Wall Propagation,” *IEE Proc.-Microw. Antennas Propag.*, Vol. 152, 581-588, 2005.
20. A. Muqaibel, A. Safaai-Jazi, “Characterization of Wall Dispersive and Attenuative Effects on UWB Radar Signals, *Journal of the Franklin Institute*, 345, 640-658, 2008.
21. Z. Yun and M. F. Iskander, “UWB Pulse Propagation through Complex Walls in Indoor Wireless Communications Environments, *2005 International Conference on Wireless Networks, Communications and Mobile Computing*, 2, 1358-1361, 2005.
22. W. Yang, Z. Qinyu, Z. Naitong, C. Peipei, “Transmission Characteristics of Ultra-Wide Band Impulse Signals,” *Wireless Communications, Networking and Mobile Computing, 2007. WiCom 2007. International Conference*, 550-553, 2007.
23. W. Yang, Z. Naitong, Z. Qinyu, and Z. Zhongzhao, “Simplified Calculation of UWB Signal Transmitting through a Finitely Conducting Slab,” *Journal of Systems Engineering and Electronics*, Vol. 19, 1070–1075, 2008.

24. A. Karousos, G. Koutitas, C. Tzaras, "Transmission and Reflection Coefficients in Time-Domain for a Dielectric Slab for UWB Signals," *Vehicular Technology Conference, 2008. VTC Spring 2008. IEEE*, 455-458, 2008.
25. P. Tewari, S. Soni, "Time-domain solution for transmitted field through low-loss dielectric obstacles in a microcellular and indoor scenario for UWB signals," *IEEE Trans. Veh. Technol. (resubmitted after 3rd revision)*, 2013.
26. A. Yahalom, Y. Pinhasi, E. Shifman, S. Petnev, "Transmission through single and multiple layers in the 3-10 GHz band and the implications for communications of frequency varying material dielectric constants," *WSEAS Trans. Commun.*, Vol. 9, 759-772, 2010.
27. R. Yao, Z. Chen, and Z. Guo, "An Efficient Multipath Channel Model for UWB Home Networking," *0-7803-8451-2/04, IEEE*, 511-516, 2004.
28. W. Yang, Z. Qinyu, Z. Naitong, C. Peipei, "Transmission Characteristics of Ultra-Wide Band Impulse Signals," *Wireless Communications, Networking and Mobile Computing, 2007. WiCom 2007. International Conference*, 550-553, 2007.
29. W. Yang, Z. Naitong, Z. Qinyu, and Z. Zhongzhao, "Simplified Calculation of UWB Signal Transmitting through a Finitely Conducting Slab," *Journal of Systems Engineering and Electronics*, Vol. 19, 1070–1075, 2008.
30. P.S.Chauhan, S.Soni and Yashu Shanker, "A Novel Approach to predict Field Strength in the Shadow of a 3-D Building Scenario," Wireless Pers Commum. (2013)
31. Z. Yun and M. F. Iskander, "UWB Pulse Propagation through Complex Walls in Indoor Wireless Communications Environments, *2005 International Conference on Wireless Networks, Communications and Mobile Computing*, 2, 1358-1361, 2005.
32. C. A. Balanis, *Advanced engineering electromagnetics*, NewYork: Wiley, 1989.
33. Paul R. Barnes, Frederick M. Tesche, " On the direct calculation of a transient plane wave reflected from a finitely conducting half space," *IEEE Transactions on the Electromagnetic compatibility, Vol,33,No.2 May 1991*
34. Robert C.Qiu,Quingchong Liu, "Physics-Based Pulse Distortion for Ultra-Wideband Signals,"
IEEE Transactions on vehicular technology, Vol, 54,No. 5, September 2005.
35. E. Oran Brigham, *The Fast Fourier Tramform. Englewood Cliffs*. NJ: Prentice-Hall, 1988.